AFWAL-TR-88-2033

DETECTION OF EXCITED STATES BY LASER-INDUCED FLUORESCENCE AND ANALYSIS OF ENERGY TRANSFER

A. B. WEDDING and A. V. PHELPS

QUANTUM PHYSICS DIVISION
U. S. BUREAU OF STANDARDS
BOULDER, CO 80303

July 1988

FINAL REPORT FOR PERIOD OCTOBER 1986 - SEPTEMBER 1987

AERO PROPULSION LABORATORY
AIR FORCE WRIGHT AERONAUTICAL LABORATORIES
AIR FORCE SYSTEMS COMMAND
WRIGHT-PATTERSON AIR FORCE BASE, OHIO 45433-6563

NOTICE

When Government drawings, specifications, or other data are used for any purpose other than in connection with a definitely Government-related procurement, the United States Government incurs no responsibility or any obligation whatsoever. The fact that the Government may have formulated or in any way supplied the said drawings, specifications, or other data, is not to be regarded by implication, or otherwise in any manner construed as licensing the holder to manufacture, use, or sell any patented invention that may in any way be related thereto.

This report has been reviewed by the Office of Public Affairs (ASD/PA) and is releasable to the National Technical Information Service (NTIS). At NTIS, it will be available to the general public, including foreign nations.

This technical report has been reviewed and is approved for publication.

Alan Garscadden

ALAN GARSCADDEN
Power Components Branch
Aerospace Power Division
Aero Propulsion Laboratory

Paul R. Bertheaud

PAUL R. BERTHEAUD, Chief
Power Components Branch
Aerospace Power Division
Aero Propulsion Laboratory

FOR THE COMMANDER

William A. Seward

WILLIAM A. SEWARD, Lt Col, USAF
Deputy Director
Aerospace Power Division
Aero Propulsion Laboratory

If your address has changed, if you wish to be removed from our mailing list, or if you are no longer employed by your organization please notify AFWAL/POOC-3, Wright-Patterson AFB, OH 45433-6563 to help us maintain a current mailing list.

Copies of this report should not be returned unless return is required by security considerations, contractual obligations, or notice on a specific document.

REPORT DOCUMENTATION PAGE

Form Approved
OMB No. 0704-0188

1a. REPORT SECURITY CLASSIFICATION UNCLASSIFIED	1b. RESTRICTIVE MARKINGS
2a. SECURITY CLASSIFICATION AUTHORITY	3. DISTRIBUTION/AVAILABILITY OF REPORT Approved for public release; distribution is unlimited
2b. DECLASSIFICATION/DOWNGRADING SCHEDULE	
4. PERFORMING ORGANIZATION REPORT NUMBER(S)	5. MONITORING ORGANIZATION REPORT NUMBER(S) AFWAL/TR-88-2033
6a. NAME OF PERFORMING ORGANIZATION Quantum Physics Division U.S. Bureau of Standards 6b. OFFICE SYMBOL (If applicable)	7a. NAME OF MONITORING ORGANIZATION Air Force Wright Aeronautical Laboratories Aero Propulsion Laboratory (AFWAL/POOC)
6c. ADDRESS (City, State, and ZIP Code) Boulder CO 80303	7b. ADDRESS (City, State, and ZIP Code) Wright-Patterson AFB OH 45433-6563
8a. NAME OF FUNDING/SPONSORING ORGANIZATION 8b. OFFICE SYMBOL (If applicable)	9. PROCUREMENT INSTRUMENT IDENTIFICATION NUMBER MIPR FY 1455-86-N0652
8c. ADDRESS (City, State, and ZIP Code)	10. SOURCE OF FUNDING NUMBERS

PROGRAM ELEMENT NO.	PROJECT NO.	TASK NO	WORK UNIT ACCESSION NO.
61102F	2301	S1	24

11. TITLE (Include Security Classification)
Detection of excited states by laser-induced fluorescence and analysis of energy transfer

12. PERSONAL AUTHOR(S)
A. B. Wedding and A. V. Phelps

13a. TYPE OF REPORT	13b. TIME COVERED	14. DATE OF REPORT (Year, Month, Day)	15. PAGE COUNT
Final	FROM Oct 86 TO Sep 87	July 1988	66

16. SUPPLEMENTARY NOTATION

17. COSATI CODES			18. SUBJECT TERMS (Continue on reverse if necessary and identify by block number)
FIELD	GROUP	SUB-GROUP	
20	5	1	hydrogen, nitrogen, metastables, electrons, radiation, excitation coefficient, excited states
20	6	2	

19. ABSTRACT (Continue on reverse if necessary and identify by block number)

Laser absorption measurements of the collisional destruction of the $H_2(c^3\Pi_u^-)$ metastable levels have been extended to include measurements of the rate coefficients and radiative lifetimes for the $H_2(a^3\Sigma_g^+)$ levels and of collisional coupling between levels of these electronic states with the same vibrational and rotational quantum numbers. The rate coefficients for quenching of the $H_2(a^3\Sigma_g^+)$ levels vary from 6 to 11 $\times 10^{-16}$ m^3/s. Collisional excitation transfer from the $H_2(a^3\Sigma_g^+)$ state to the $H_2(c^3\Pi_u^-)$ state accounts for most if not all of this destruction. The absorption technique was also applied to the a" $^1\Sigma_g^+$ metastable state of N_2. A preliminary rate coefficient for quenching to lower electronic states is 2 $\times 10^{-16}$ m^3/s. A complete analysis will require that the observed collisional coupling among the rotational levels of the a" $^1\Sigma_g^+$ be taken into account.

20. DISTRIBUTION/AVAILABILITY OF ABSTRACT	21. ABSTRACT SECURITY CLASSIFICATION
☒ UNCLASSIFIED/UNLIMITED ☐ SAME AS RPT. ☐ DTIC USERS	Unclassified

22a. NAME OF RESPONSIBLE INDIVIDUAL	22b. TELEPHONE (Include Area Code)	22c. OFFICE SYMBOL
A. Garscadden	(513) 255-2923	AFWAL/POOC

DD Form 1473, JUN 86 *Previous editions are obsolete.*

PREFACE

This work was performed in the Quantum Physics Division, U.S. Bureau of Standards, at the Joint Institute for Laboratory Astrophysics under MIPR FY1455-86-NO652. The work was performed during the period October 1986 through September 1987 under Project 2301 Task S1, Work Unit 24. The Air Force contract manager was Dr. Alan Garscadden, Energy Conversion Branch, Air Force Wright Aeronautical Laboratories, Aero Propulsion Laboratory, WPAFB, OH 45433-6563.

TABLE OF CONTENTS

LIST OF ILLUSTRATIONS

LIST OF ILLUSTRATIONS (Continued)

FIGURE PAGE

LIST OF ILLUSTRATIONS (Concluded)

FIGURE PAGE

LIST OF TABLES

SECTION I

INTRODUCTION

The objective of this research is to develop diagnostics and models required for measurement and prediction of the properties of electrical discharges in molecular gases. Discharges in molecular gases are important in Air Force technology because of their use in devices such as plasma processors, high power switches, and negative ion sources and because of their role in phenomena such as corona and lightning. The research program includes; a) the development and application of laser fluorescence and absorption techniques to the measurement of excited state densities in electric discharges, b) the measurement of the properties of the excited states of importance in molecular discharges of current interest, c) the application of various diagnostic techniques to the determination of the characteristics of moderate current density, transient electrical discharges, and d) the quantitative comparison of these results with appropriate discharge models. During the past year we have (a) made measurements of the collisonal and radiative destruction of the $a^3\Sigma_g^+$ state, (b) completed measurements and analyses of the collisional coupling of H2 molecules in the $c^3\Pi_u^-$ state with the nearby $a^3\Sigma_g^+$ radiating state, and c) extended the absorption technique to the a" $^1\Sigma_g^+$ metastable state of N_2. The properties of metastable H2 are of current interest because of the use of discharges in H2 as switching devices (thyratrons), as negative ion sources, and as infrared lasers. The properties of the a" $^1\Sigma_g^+$ metastable state of N_2 are of current interest because they represent an energy reservoir in N_2 discharges and because of the proposal that they play an important role in the growth of instabilities in high power N_2-CO_2 lasers.

The collisional quenching rate constant for the $c^3\Pi_u^-$ (v=2, N=1) level was first determined by Tischer and Phelps[1] under a earlier part of the program. A paper describing measurements under this program of the collisional quenching rate coefficients for a range of rotational and vibrational levels of the $c^3\Pi_u^-$ state has just been submitted to the Journal of Chemical Physics.[2] This paper also contains much of the material presented in Sections II and III of this report. Although some of this material was contained in last year's report,[3] it is repeated for clarity of presentation.

Section II of this report describes the experimental technique used in this work. Measurements and analyses of the collisional and radiative lifetimes of the $a^3\Sigma_g^+$ state are reported in Section III B, while the results of measurements of the rate coefficients for collisional coupling of the $a^3\Sigma_g^+$ and $c^3\Pi_u^-$ states are presented in Section III C. Measurements of the rate coefficients for quenching and rotational coupling for the a" $^3\Sigma_g^+$ metastable state of N_2 are presented in Section IV. The status of measurements of the electric field strength to gas density ratio E/n for our discharges in N_2 and their comparison with theory are summarized in Section IV F.

In this report we will often refer to the $H_2(c^3\Pi_u^-)$, the $H_2(a^3\Sigma_g^+)$, and the N_2(a" $^3\Sigma_g^+$) states as the a, c, and a" states, respectively.

SECTION II

EXPERIMENTAL TECHNIQUE

The rate constants for quenching and collisional coupling of the $c^3\Pi_u^-$ and $a^3\Sigma_g^+$ states of H_2 and for the various rotational levels of the a" $^3\Sigma_g^+$ state of N_2 were determined using a laser absorption technique developed by Bethune, Lankard, and Sorokin[4] and extended by Tischer and Phelps[1] and Wedding and Phelps.[2] In this report we will first describe the technique in terms of its application to the levels of the $c^3\Pi_u^-$ and $a^3\Sigma_g^+$ states of H_2 and then describe any important differences applicable to the $N_2(a''\ ^3\Sigma_g^+)$ state.

The $H_2(c^3\Pi_u^-)$ metastables were generated by electron excitation of ground state molecular hydrogen in a pulsed discharge. This population was then depleted by pulsed laser excitation to higher levels of H_2 which can radiate to the dissociating $b^3\Sigma_u^+$ state. The pulsed laser excitation was timed to occur during a period of constant electronic excitation, i.e., quasi steady-state discharge current and c-state density. The collisional quenching rate coefficient was determined from the time constant of recovery of the c state density after depletion by the pulsed laser. The c state density was monitored by cw laser absorption of appropriate H_2 spectral lines. See Section III A for a discussion of the absorption spectra.

A pulsed discharge of 3 to 5 μs duration and up to 4 A at 10 Hz generated a $c^3\Pi_u$ density which was probed using an optically balanced cw laser absorption arrangement shown in Figure 1. The difference in the signals from the two fast photodiode detectors (<1 ns response) is proportional to the absorption by the electronically excited species in the discharge volume. This system has the two-fold advantage of suppressing the intensity

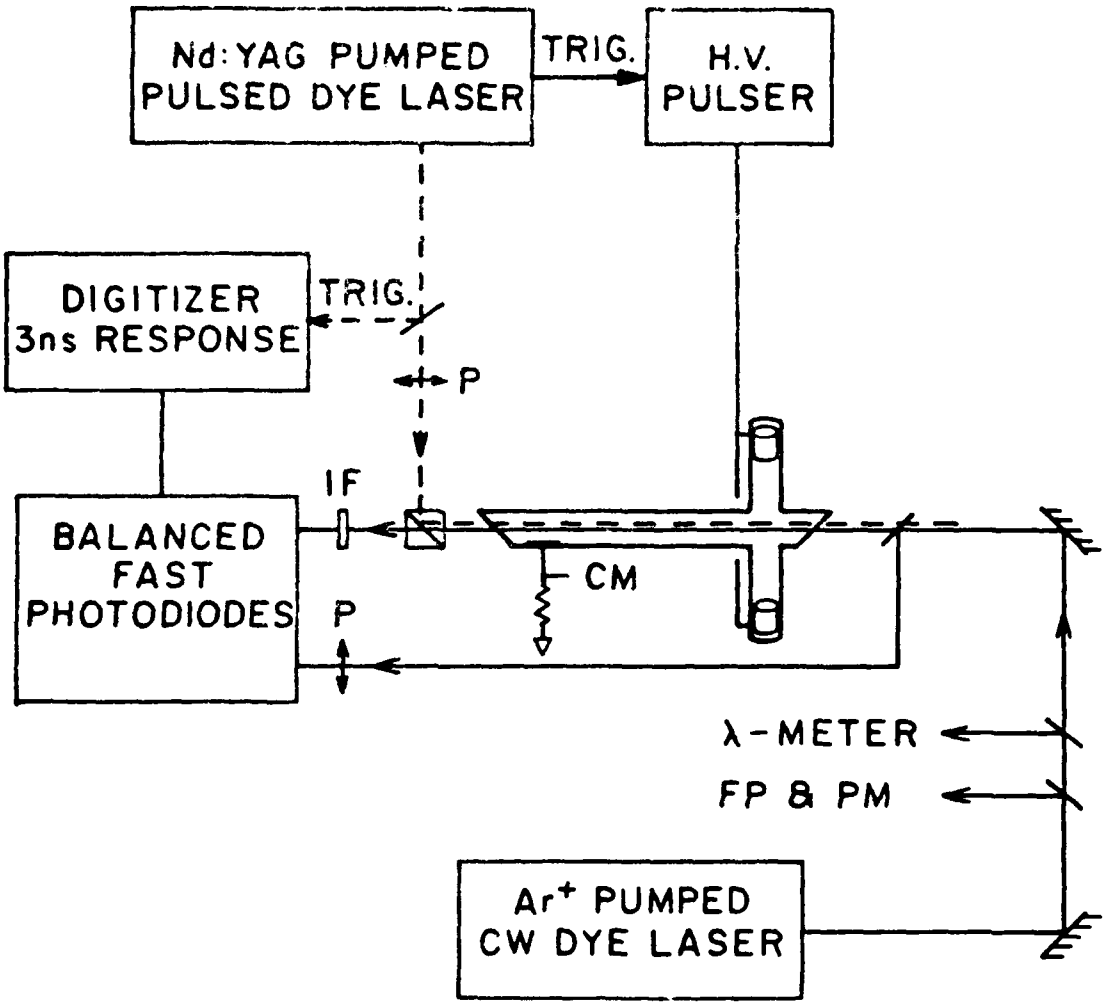

Figure 1. Schematic of the experimental configuration used for the collisional coupling measurements in H_2 and for collisional quenching and coupling measurements in N_2.

fluctuations of the cw laser and removing the dc level associated with the incident laser intensity. The difference signal was amplified and then input to a transient digitizer (≈ 1 ns resolution) where it was averaged and then transferred to a computer for analysis. The time resolution of the system was limited by the diode preamplifier and was less than 3 ns. Linearity of the detection system was demonstrated using neutral density filters. Typically, averages of 2000 transients gave a good signal-to-noise ratio.

A schematic of the discharge tube is shown in Figure 1. Here we provide two cathodes in side arms in order to remove the cathode region from the absorption path and allow the measurement of absorption by metastables only within the positive column of the discharge. The cathode fall region was confined to within the off-axis portion of the tube. The probed on-axis length of positive column was 200 mm. Aluminum electrodes were used to minimize sputtering. Observations of the discharge sidelight with an apertured photomultiplier showed the absence of striations prior to and during the measurement period. Because of the short c- and a-state lifetimes gas impurity effects could be neglected. Published measurements[5] and our measurements and calculations of the discharge maintenance conditions for H_2 yielded electric field to gas density ratios E/n of 85 to 115 Td (1 Td = 10^{-21} V m^2), average electron energies $\langle\epsilon\rangle$ of ~ 3 eV, and electron densities n_e of 10^{18}xI m^{-3}, where I is the discharge current in amperes. The energy input to the gas during the discharge pulse prior to the measurement was approximately 0.03xI eV/molecule. Calculations based on the rate coefficients of Buckman and Phelps[6] yielded a translational temperature rise[7] of less than 75xI K, a rotational temperature rise of about 15xI K, a fractional excitation to the first vibrational level of about 0.01xI, and a fractional dissociation of

about 0.006xI. The repetition rate of 10 Hz ensured that between pulses the translational, rotational, and vibrational temperatures returned to the wall temperature. The recombination of dissociated atoms depends critically on the wall conditions which were unknown in our experiment. Measurements in similar discharge tubes[8] suggest sufficiently fast wall recombination to prevent significant carry-over of the H atom density. Because of the short a- and c-state lifetimes, we do not expect quenching by H atoms to be significant.

For the series of collisional quenching experiments the cw probe laser and the pulsed pump laser were tuned to two different absorption transitions from the same lower state. The two laser beams counter propagated through the discharge tube and were slightly non-collinear to avoid coupling between the two laser cavities. The diameter of the pulsed pump beam was kept large, 4 mm diameter, to provide a more nearly uniform radial and longitudinal spatial distribution of perturbed molecules. The diameter of the cw beam was less than that of the pulsed beam to ensure good spatial overlap with the depleted molecules. The Nd:YAG pumped pulsed dye laser line width was determined by optogalvanic detection of a Ne absorption signal with a highly attenuated intensity and found to be about 20 GHz FWHM. A 5 ns pulsed laser flux of 50 W mm^{-2} incident on the discharge yielded a highly saturated depletion signal corresponding to between 30 percent and 50 percent depletion of the $c^3\Pi_u^-$ state population for the stronger absorption lines. For the c-state quenching experiments, the Ar^+ pumped cw dye laser was operated in a multi-mode configuration (line width 7 GHz FWHM). The beam was attenuated so that only about 0.5 mW was incident upon the discharge volume as the transitions studied here are easily saturated.[1] Since the Doppler broadened absorption line width

was 4.4 GHz and the observed absorption was less than 15 percent, the peak absorption was proportional to the excited state density.

For the investigations of collisional coupling in H_2 discussed in Section III C, the cw laser was operated single mode, and a multi-pass configuration was used to increase the absorption length probed. The beam was reflected seven times between plane mirrors mounted externally to the discharge tube. The pulsed pump laser was directed to counter propagate through the discharge volume three times in such a way as to avoid detection of reflected pulsed laser flux and cavity coupling. The two laser beams were of orthogonal polarization in the interaction region and a polarization selector was used to discriminate against the pulsed laser component before detection. This multi-pass configuration resulted in an increase in the percentage absorption and some reduction in the percentage depletion due to a reduced overlap of the two beams. Overall, the ability to detect small density changes was enhanced. These experiments were greatly aided by the use of a relatively inexpensive, direct reading λ-meter[9] accurate to 0.004 nm. The λ-meter was calibrated against an I_2 absorption spectra which is known to 0.002 cm^{-1}.

Metastables in the a"-state of N_2 were generated in a pulsed discharge and probed using modifications of the laser absorption technique just described for H_2 metastables. The discharge tube consisted of the cross shaped pyrex vessel shown schematically in Figure 1. In order to increase the laser absorption path length the cw laser beam was retroreflected along the axis of the tube between plane mirrors mounted externally to the tube. For the results presented here the effective absorption length was 1.8 m. The cw laser was arranged in an optically balanced configuration as shown in Figure 1. The difference signal between the two detected cw laser intensities is

directly proportional to the absorption within the discharge tube. The cw laser power within the discharge volume was less than 0.5 mW and the intensities were detected using fast (< 1 ns) photodiodes. This signal was then amplified and recorded using a transient digitizer which is triggered from the laser pulse. The absorption transients were then averaged, typically 3000 times to obtain good signal to noise, and then transferred to a computer for analysis. Typical absorption data for N_2 metastables will be presented in Section IV.

The destruction of excited species by metastables and impurities in nitrogen systems is of some concern.[10] The discharge tube was connected to a large (~ 40 liters) stainless steel vacuum vessel which acted as a gas reservoir. The system could be baked at 120 K and had a base pressure of < 1.3×10^{-4} Pa. No change of the destruction frequencies was detected as a function of gas residence time or when the system was flushed with pure N_2 between individual measurements.

III. H_2 METASTABLE-RADIATING STATE COLLISIONAL COUPLING

The lifetimes of the rotational and vibrational levels of the $c^3\Pi_u$ state of H_2 in the absence of collisions have been the subject of many experimental measurements[11,12] and theoretical calculations.[13,14] The radiative lifetimes for rotational levels which do not predissociate are of the order of 1 ms for the v=0 vibrational level via the forbidden magnetic dipole transition to the $b^3\Sigma_u^+$ state and approximately 100 μs for higher vibrational levels which can radiate to the nearby $a^3\Sigma_g^+$ state. Hence its metastable label. On the other hand, the $a^3\Sigma_g^+$ state radiates[15–17] in about 10 ns to the $b^3\Sigma_u^+$ state. While prior to this series of experiments very little information was available as

to the collisional destruction of the c state,[18] the experimental determinations[15,19] of the destruction rate coefficients for the a state were in serious disagreement.

Interest in the a and c states of H_2 is evidenced by the observation[20] of molecular hydrogen laser lines in the vicinity of 3.8 μm which were assigned to $a^3\Sigma_g^+ \rightarrow c^3\Pi_u$ transitions; by proposals[3,21] that the c state is important in hydrogen thyratrons and can be used for laser energy storage; by the observation[2] that the collisional destruction of the c state is very rapid; by studies[22,23] of the production of c-state molecules in high energy H_2 collisions; and by the measurements[24] of cross sections for c and a states by electron beam excitation. The collisional kinetics of the $c^3\Pi_u$ and $a^3\Sigma_g^+$ levels are also of interest because of the information they can yield regarding the potential energy curves for H_2-H_2 complexes.[25] Finally, we note that the c state has been proposed[26] to play a role in the production of negative ions in low pressure H_2 discharges.

We adopt the convention[23] of designating as Π^+ states the levels of the $c^3\Pi_u$ state resulting from Λ-doubling and having the same parity as the Σ^+ states. These levels of the $c^3\Pi_u^+$ state predissociate in about 10^{-9} s, via rotational coupling to the dissociating $b^3\Sigma_u^+$ state.[11-14] On the other hand, the $c^3\Pi_u^-$ levels do not predissociate rapidly and radiate slowly to the nearby a state as indicated above.

A. Absorption spectra and absorption transients

The strongest lines of the visible (570 - 640 nm) absorption spectrum were the Q transitions to the $g^3\Sigma_g^+$ state and R transitions to the $i^3\Pi_u$ and $j^3\Delta_g$ states from the lower rotational and vibrational levels of the $c^3\Pi_u^-$

state, where N = 1 to 3 and v = 0 to 3. Figures 2 and 3 show the levels relevant to this study. Accurate wavelengths were taken from Dieke.[27] All levels of the upper 3d states, i.e., the $g^3\Sigma_g^+$, $i^3\Pi_u$, and $j^3\Delta_g$ states, examined by Eyler and Pipkin[28] have radiative lifetimes to the $c^3\Pi_u$ state and dissociating $b^3\Sigma_g^+$ state of less than 15 ns. Upon laser excitation some of the metastables are removed from the initial c level through excitation to 3d levels and subsequent reradiation to other rotational levels of the c state and to the repulsive $b^3\Sigma_g^+$ state. The branching ratio to the lower states is unknown. Representative radiative transitions for the excited 3d levels are shown in Figure 2. The strong absorption lines yielded about 15 percent absorption of the cw laser intensity. The c-state density estimated from the metastable production[6] and loss rates was $2 \times 10^{14} \times I\ m^{-3}$. We have not been able to find or determine absolute absorption coefficients for any of the transitions used.

Figure 4 shows an example of a $c^3\Pi_u^-$ absorption and depletion transient. The upper trace shows the absorption resulting when the discharge current pulse is about 4 μs in length and 2.5 A in peak current. The lower trace shows the depletion waveform produced by the pulsed laser and the exponential curve fitted to the recovery portion of the data. The analysis of this and similar $c^3\Pi_u^-$ waveforms for other levels and for other H_2 densities and discharge currents has been covered in a previous report.[3]

The time variation of the $a^3\Sigma_g^+$ density was monitored by observing absorption of lines of the $d^3\Pi \leftarrow a^3\Sigma_g^+$ or Fulcher band system.[29] In most cases we used R-branch transitions, although for v = 1, N = 2 we used the Q branch in order to avoid an overlapping line. The absorption transients for

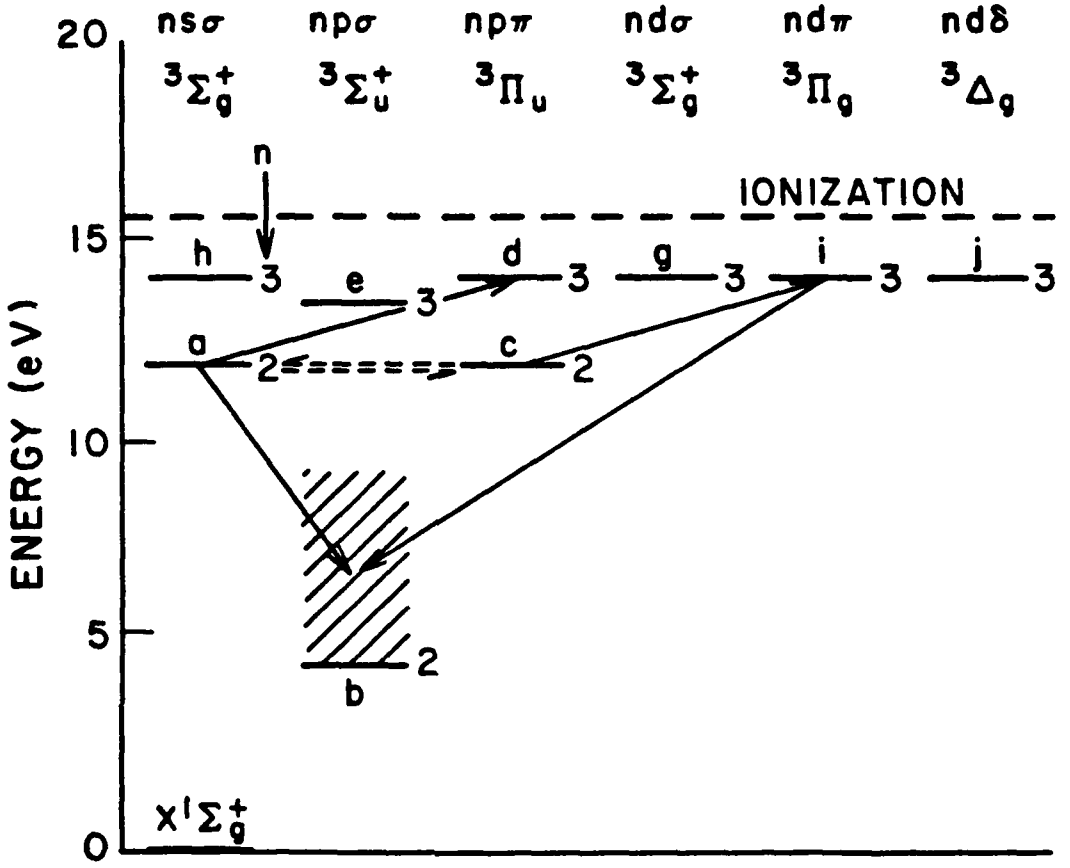

Figure 2. Energy level diagram of the relevant states of the triplet system of H_2 showing transitions of interest in this report. The dashed lines represent the collisional excitation transfer between levels of the $a^3\Sigma_g^+$ and $c^3\Pi_u^-$ states.

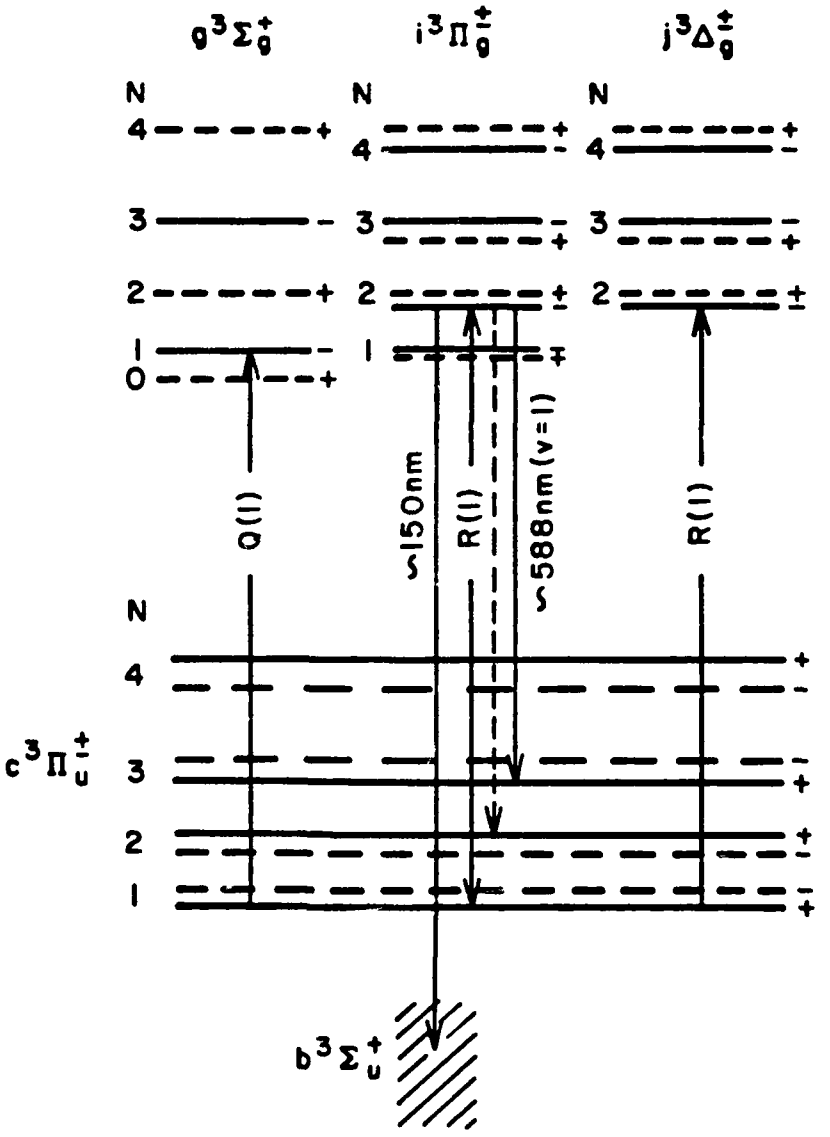

Figure 3. Schematic of the lower rotational levels for the principal states of interest. The solid lines denote ortho-H_2 and the dashed para-H_2. The upper level of the two $c^3\Pi_u$ Λ-doublet components with parity $(-1)^N$ predissociates and is denoted by $c^3\Pi_u^+$. The lower level in this schematic, denoted by $c^3\Pi_u^-$, is metastable and is studied in this work. The energy levels are not to scale and the order of the doublets varies with v.

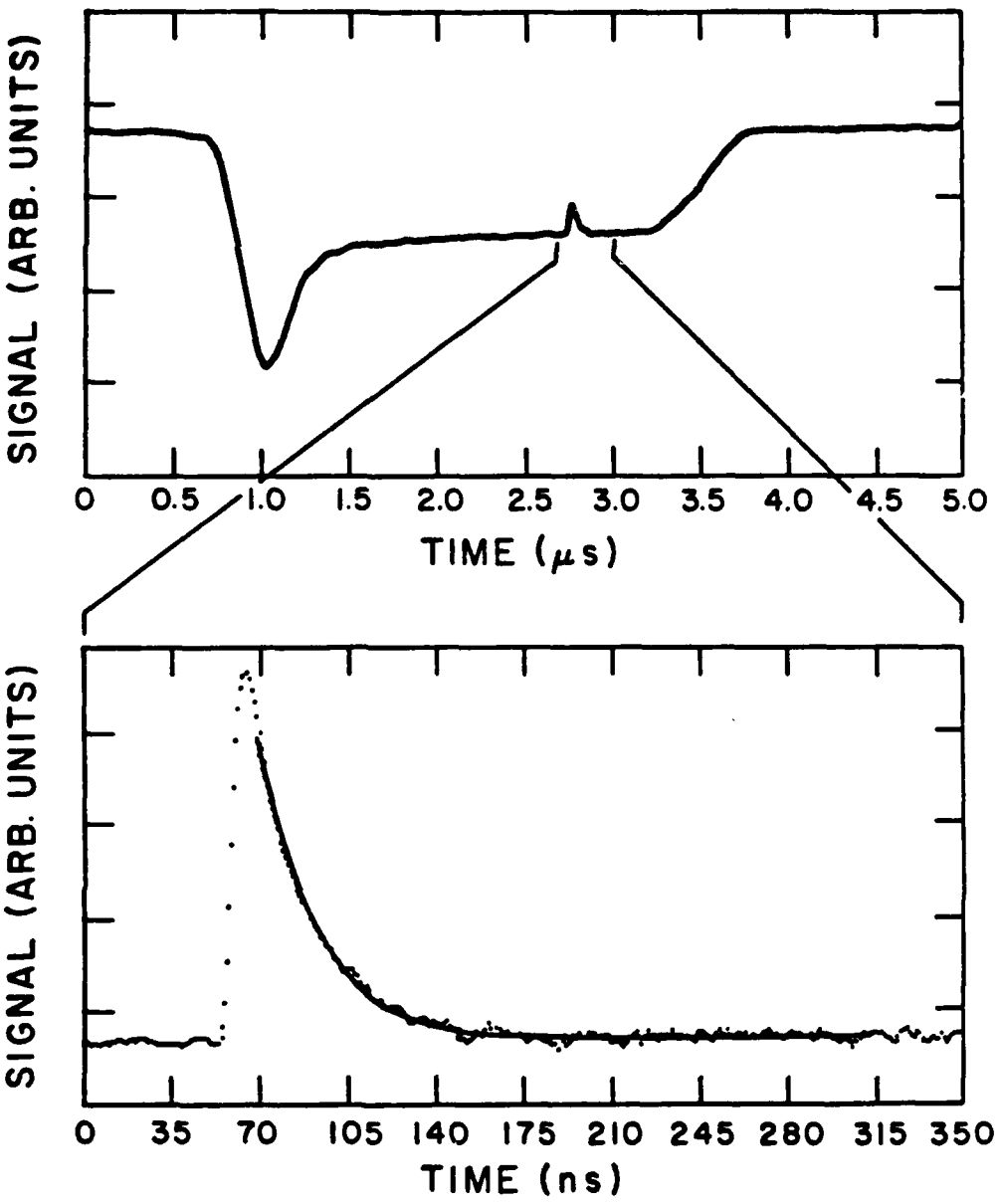

Figure 4. Absorption waveforms showing the quasi steady-state $c^3\Pi_u^-$ density during the discharge pulse, and the fit of a single exponential to the recovery of the $c^3\Pi_u^-$ (v = 0, N = 1) population after pulsed laser excitation. $n = 1.9 \times 10^{22}$ m^{-3} and I = 2.5 A. Both waveforms were taken with the single pass system.

the $a^3\Sigma_g^+$ state are very much like that shown in Figure 4, except for a faster recovery of the depletion transient and a lower signal-to-noise ratio. We see no evidence of component of the recovery at the time constant characteristic of the radiative decay of the $d^3\Pi$ state. Recent experiments[29] give radiative lifetimes of the $d^3\Pi$ state which vary from 30 to 40 ns.

B. $H_2(a^3\Sigma_g^+)$ collisional quenching measurements.

The simplified rate equation for the $a^3\Sigma_g^+$ state population, A(t), in which we neglect collisional transfer to and from other levels is

$$\frac{dA(t)}{dt} = k_{ea} n_e n - \nu_a A(t) - \sigma_a F(t)[A(t) - gD(t)] + A_{da} D(t), \quad (1)$$

where k_{ea} is the electron excitation rate for the particular $a^3\Sigma_g^+$ level of interest, n_e is the electron density and n is the H_2 density. The total rate of loss of the a-state level by radiation and by excitation transfer is proportional to the destruction frequency ν_a. The fourth term on the RHS of Equation (1) represents the laser excitation of the $a^3\Sigma_g^+$ level to an upper level of density D(t). The effective cross section for absorption of the pulsed laser flux F(t) is σ_a and the statistical weight ratio for the levels is r. The fifth term represents spontaneous emission back to the $a^3\Sigma_g^+$ state where A_{da} is the Einstein coefficient. Excitation transfer will considered in Section III C.

If we assume that the rate of excitation of the c state by electrons is constant and neglect radiative contributions from the upper excited level, the solution to Equation (1) after the laser flux has returned to zero is

$$A(t) = k_{ec} n_e n/\nu_a - \Delta A \exp(\nu_a t). \quad (2)$$

Here ΔA is the depletion of $a^3\Sigma_g^+$ density produced by the pulsed laser. The time constant for recovery of the $a^3\Sigma_g^+$ population is then $1/\nu_a$. A least-squares fit of a single exponential to recovery data similar to that shown in Figure 4 for the c state was used to obtain ν_a. Under these experimental conditions a typical a-state recovery time of ~ 10 ns was observed. The good agreement between this simple model and the experiment indicates little or no contribution of reradiation from the upper excited level, i.e., the term $A_{da}A(t)$ in Equation (1) is small over the period of the fitting which begins about 10 ns after the laser pulse. The agreement also indicates that the collisional coupling is weak.

In order to eliminate the effects of quenching by electrons, excited molecules, atoms, or other products of the discharge and possible discharge induced index of refraction effects,[30] destruction frequencies were obtained for a range of discharge currents and pressures. To obtain the collisional quenching rate coefficient k_{qc} for a particular $a^3\Sigma_g^+$ level, a linear dependence of the destruction frequencies ν_a on discharge current I and gas density was assumed, i.e.,

$$\nu_a = aI + k_{qc}n. \qquad (3)$$

We have determined the collisional quenching rate coefficient for the $a^3\Sigma_g^+$ (N = 1, v = 0 and 1) levels. The destruction frequencies ν_a determined by fitting an equation of the form of Equation (2) to the measured recovery of transmission waveforms for the v = 1, N = 1 level are plotted versus H_2 density in Figure 5. In this case no current dependence of the total destruction frequencies was observed within the uncertainty of the

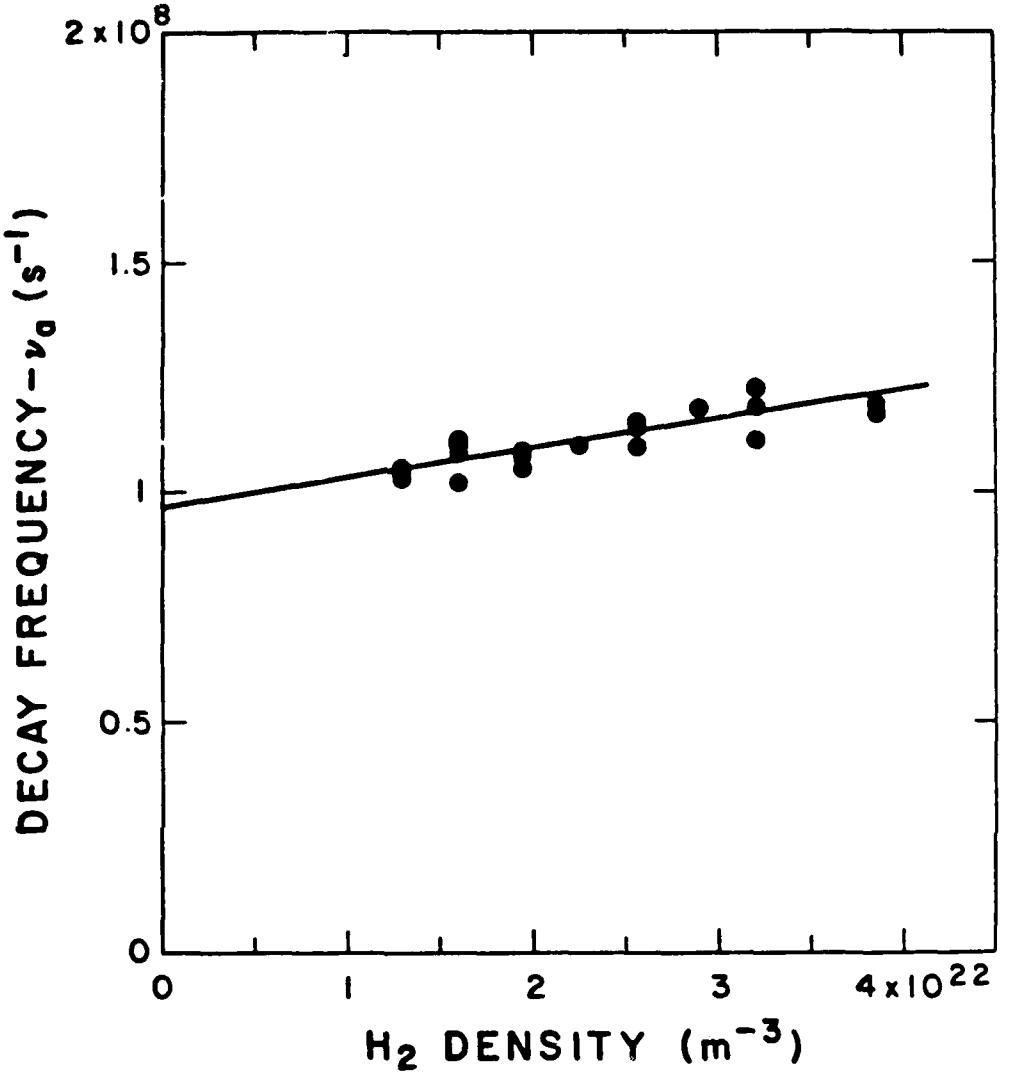

Figure 5. Fit of a linear dependence of the destruction frequencies on gas density for the $a^3\Sigma_g^+(v = 1, N = 1)$ level of H_2. The current was 1 A.

Table 1. $H_2(a^3\Sigma_g^+)$ collisional quenching rate coefficients k_{qa}, and radiative lifetimes τ_a for the N=1 rotational levels.

v	k_{qa} (10^{-16} m^3s^{-1})	τ_a (10^{-9} s)	$k_{qa}\tau_a$ (10^{-24} m^3)
0	11.5±1.0	11.1±0.3	12.8
1	6.3±0.8	10.4±0.3	6.6

measurements. The linear density dependence of the destruction frequencies then yielded the collisional quenching coefficients k_{qa} given in Table 1. The zero density intercepts of plots such as in Figure 5 yield the a-state lifetimes τ_a for the $a^3\Sigma_u^+ \rightarrow b^3\Sigma_g^+$ radiative transition. They are listed in Table 2. We obtain radiative lifetimes for N = 1 levels of the v = 0 and 1 states which are somewhat longer than 10 ns. Rotationally averaged radiative lifetimes for given vibrational levels for these transition have most recently been measured[16] to be slightly less than 10 ns. The agreement of the absolute values and the variation with vibrational level of our results with the recent theoretical results of Kwok et al.[17] and the earlier experimental data[16] is very good.

Our state selected quenching coefficients (Table 1) show a strong dependence on vibrational level. Previous lifetime measurements versus gas density for the a state[15] yielded collisional quenching rate coefficients ranging from 5×10^{-17} to 1.8×10^{-16} m^3 s^{-1}. These values are considerably below our values. Other measurements[19] of a-state quenching were based on the analysis of the relative intensity of $a^3\Sigma_g^+ \rightarrow b^3\Sigma_g^+$ UV emission as a function of H_2 density normalized to a constant production rate. These results are most accurately described in terms of the product of the collisional quenching rate coefficient and the radiative lifetime, $k_{qa}\tau_a$. Center[19] obtained a value 5.3×10^{-24} m^3, which is somewhat lower than our results. Recently, this product was measured by Tischer and Phelps[30] using an analysis of the $a^3\Sigma_g^+ \rightarrow b^3\Sigma_u^+$ radiation emitted from a drift tube.[31] They obtained a value of $(8.2 \pm 2.0) \times 10^{-24}$ m^3, which was independent of the wavelength used. The uncertainty cited reflects uncertainties in the spatial dependence of the efficiency for detection of the radiation. At the wavelengths they used (253

Table 2. Determination of collisional coupling among a- and c-state levels. The fractional absorption and depletion are given as a percentage of the incident cw laser intensity. All transitions are $\Delta v=0$. Wavelengths are vacuum values. The H_2 density was 1.61×10^{22} m^{-3} and the current was 1.5 A.

Perturbed level[a]			Observed level and λ			Signal	
v	N	λ(nm)	state	N	λ(nm)	%abs.	%dep.
0	1	581.421	c	1	593.300(Q-g)[b]	6.6	2.8
			a	1	601.996(Q-d)	4.7	0.12
1	1	602.291	c	1	588.978(R-i)	13.6	2.7
			a	0	609.992(R-d)	na[d]	none[d]
			a	1	608.246(R-d)	5.1	0.5
			a	2	612.894(Q-d)	na	none
			a	3	606.496(R-d)	na	none
1	2	605.492	c	2	588.628(R-i)	2.9	0.5
			a	--[c]	--	na	none
1	3	598.088	c	3	588.556(R-i)	5.0	0.4
			a	--[c]	--	na	none

[a] Only $c^3\Pi_u^-$ state levels were perturbed in these measurements.

[b] The parentheses following the wavelengths give the rotational branch and the designation of the upper electronic state.

[c] Observations made for all a state levels listed for the v = 1, N = 1 levels of the c state.

[d] The entry of none means that the collision induced depletion was less than 0.1 percent. The na indicates that when no coupling effect was observed the absorption signal was not recorded.

and 285 nm) significant contributions from several vibrational levels occur.[17] An average of our values agrees well with their result.

We made a limited set of measurements of the lifetimes for various rotational levels of the $a^3\Sigma_g^+(v = 0)$ state at a H_2 density of 1.61×10^{22} m^{-3} and a current of 1.5 A. The resultant total destruction frequencies for N = 0, 2, and 3 were from 60 percent to 120 percent of the value for N = 1.

C. $H_2(a^3\Sigma_g^+)$ to $H_2(c^3\Pi_u^-)$ excitation transfer

The rate coefficient for collisional excitation transfer or coupling between the N=1 levels of the $a^3\Sigma_g^+$ and $c^3\Pi_u^-$ states has been determined by measuring and analyzing changes in the population of $a^3\Sigma_g^+$ levels when the $c^3\Pi_u^-$ density is depleted and vice versa. The a-state population is monitored by cw laser absorption to the $d^3\Pi_u$ state as shown in Figure 2. Figure 6 shows the relation between the lower rotational levels for the a and c states for v = 0 and 1 levels as calculated from the term-value data of English and Albritton.[32]

1. Search for excitation transfer

The results of the search for excitation transfer between the c and a states are summarized in Table 2. As indicated by the entries in the last column of Table 2 and by the dotted arrows in Figure 6, excitation transfer from the c state to the a state was observed for the N=1 levels of the v = 0 and 1 states. Data for this and the inverse process will be analyzed in detail in Section III C3. No indications of excitation transfer to the other levels listed in Table 2 were observed.

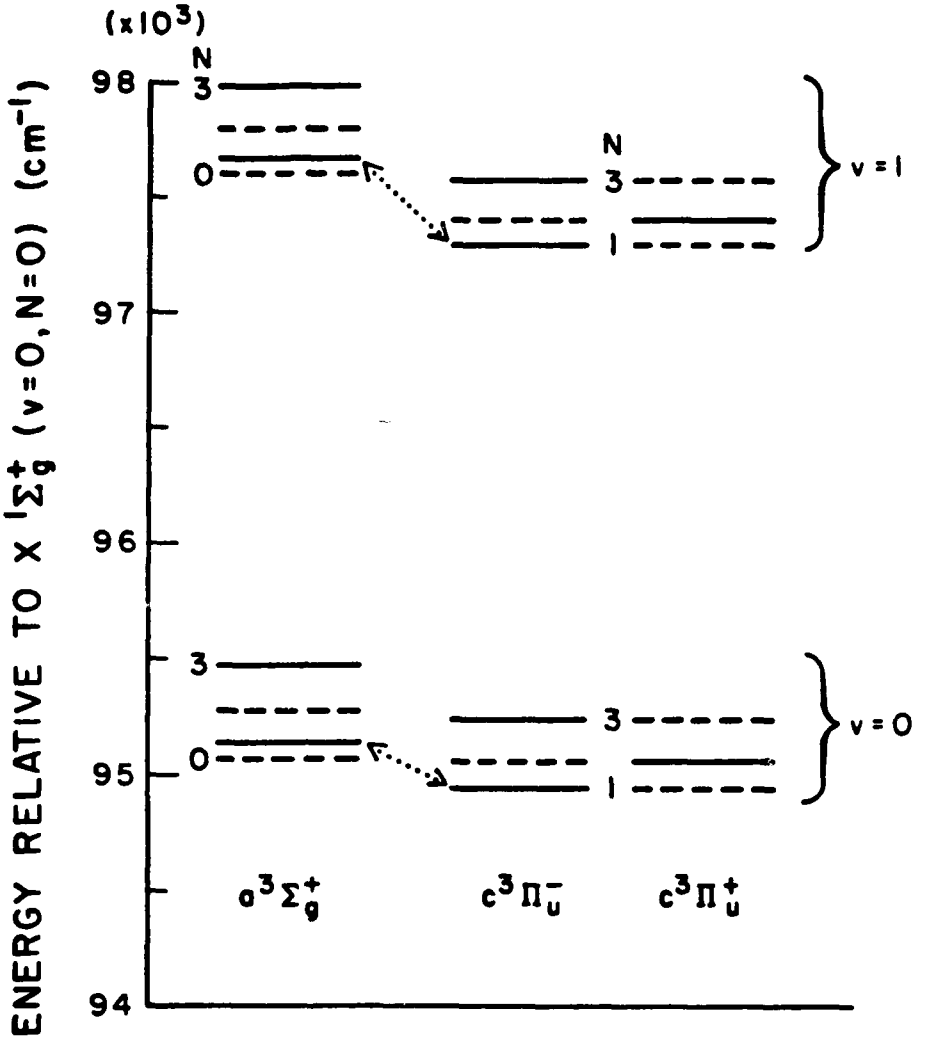

Figure 6. The energy relationships between the lower rotational levels of the $c^3\Pi_u$ and $a^3\Sigma_g^+$ states for v = 0 and 1. The solid lines denote ortho-H_2 and dashed para-H_2. The dotted line shows the observed excitation transfer.

Failure to observe excitation transfer between the levels of the $c^3\Pi_u^-$ state with odd N and the levels of the a state with even N is attributed to the difficulty of ortho-para conversion by H_2. Similarly, for the levels ofthe $c^3\Pi_u^-$ state with even N and the levels of the a state with odd N. Failure to observe excitation transfer between the N = 2, v = 1 levels of the c and a states is initially surprising. However, the absence of such observations seems more reasonable when one notes (a) the factor of 4.7 smaller absorption signal for N = 2 levels than for N = 1 levels of the c state indicating a much lower N = 2 density than N = 1 density, (b) unknown but probably comparable absorption cross sections for the Q and R branch transitions[27] used in Table 2, and (c) the low signal-to-noise indicated by the best-case waveform shown in Figure 7. Arguments (1) and (3) also apply to the N = 3, v = 1 levels. No data was obtained for the v = 0, N = 2 and 3 levels, for which the absorption signals were quite small. Indications that energy differences are not the dominant factor in determining the probability of excitation transfer are the observations of comparable signals from transfer between the c and a states for the v = 0 levels and for the v = 1 levels. Excitation transfer from the c- or a-state levels in $\Delta N = 1,3,..$ transitions conserving nuclear spin would result in transfer to the rapidly predissociating $c^3\Pi_u^+$ states shown in Figure 7 and would not be observed.

2. Determination of rate coefficients

If we now consider a model of the $c^3\Pi_u^-$ and $a^3\Sigma_g^+$ states including collisional excitation transfer between them, then the rate equations for the period following the laser pulse can be expressed as

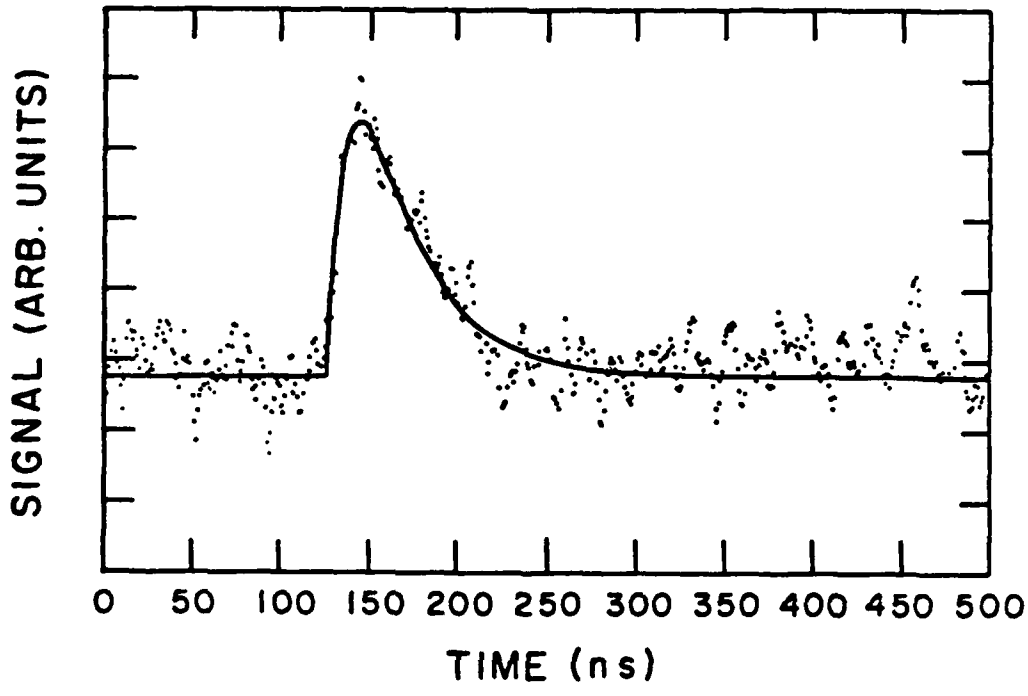

Figure 7. Collision-induced depletion of the $a^3\Sigma_g^+(v = 1, N = 1)$ level of H_2 resulting from laser-induced depletion of the $c^3\Pi_u^-(v = 1, N = 1)$ level of H_2. The current was 1 A.

$$dC(t)/dt = k_{ec}n_e n + k_{ac}nA(t) - (k_{qc} + k_{ca})nC(t) \qquad (4)$$

and

$$dA(t)/dt = k_{ea}n_e n + k_{ca}nC(t) - (A_a + k_{qa}n + k_{ac}n)A(t) \quad , \qquad (5)$$

where k_{ac} is the excitation transfer rate coefficient from state a to state c, k_{ei} is the electron excitation rate coefficient to state i, A(t) is the $a^3\Sigma_g^+$ population, and A_a is the spontaneous emission coefficient from the $a^3\Sigma_g^+$ state. As in Equations (1) and (2), we neglect reradiation from the upper state of the pump transition and radiative decay of the c state.

We are interested only in the perturbation solution and hence may ignore the constant source terms in Equations (4) and (5). Applying the basic assumption that the ground state population is not a function of time, i.e., C(t) and A(t) << n, we see that the solutions describing the time rate of change of the $a^3\Sigma_g^+$ and $c^3\Pi_u$ state populations are given by

$$C(t) = \frac{(\nu_a C_0 + \nu_{ac} A_0)(e^{-\beta t} - e^{-\alpha t}) + C_0(\alpha e^{-\alpha t} - \beta e^{-\beta t})}{(\alpha - \beta)} \qquad (6)$$

and

$$A(t) = \frac{(\nu_c A_0 + \nu_{ca} C_0)(e^{-\beta t} - e^{-\alpha t}) + A_0(\alpha e^{-\alpha t} - \beta e^{-\beta t})}{(\alpha - \beta)} \quad , \qquad (7)$$

where

$$\nu_c = (k_{qc} + k_{ca})n, \qquad \nu_{ac} = k_{ac}n,$$

$$\nu_a = (A_a + k_{qa}n + k_{ac}n), \qquad \nu_{ca} = k_{ca}n,$$

and $-\alpha$ and $-\beta$ are the roots of the equation $s^2 + s(\nu_c + \nu_a) + (\nu_c\nu_a - \nu_{ac}\nu_{ca}) = 0$. The initial density perturbations of the a and c states are A_0 and C_0, respectively. We are particularly interested in these solutions when either A_0 or C_0 is zero. Thus, when $A_0 = 0$

$$C(t) = \frac{C_0[(\alpha - \nu_a)e^{-\alpha t} - (\beta - \nu_a)e^{-\beta t}]}{(\alpha - \beta)} \qquad (8)$$

and

$$A(t) = \frac{C_0\nu_{ca}(e^{-\beta t} - e^{-\alpha t})}{(\alpha - \beta)} \quad . \qquad (9)$$

The small depletion of the $a^3\Sigma_g^+$(v=0, N=1) level resulting from depletion of the $c^3\Pi_u^-$(v=0, N=1) level by pulsed laser excitation is shown in Figure 7 and has the temporal behavior expected from Equation (9). A fit of Equation (9) to the a-state depletion signal is shown as a solid line. The increase in depletion is dominated by the shorter time constant of $1/\alpha$ = 11 ns, which is approximately equal to that for a-state destruction (Section III B). The signal has a final recovery time constant equal to that for the c-state levels under identical experimental conditions, i.e., $1/\beta$ = 33 ns. The time dependence of the a state depletion signals for N = 1, v = 0 and for N = 1, v = 1 resulting from excitation transfer from their respective c-state levels are very similar.

We have also looked at the current and pressure dependence of the amplitude factor in Equation (9). In order to evaluate the magnitudes of these weak coupling signals, fits of Equation (9) were performed using previously determined values for the two time constants α and β. No current dependence of the amplitude was observed. For electrons to account for the excitation transfer to the a state their rate coefficient would have to be about 10^{-11} m^3 s^{-1}, an extremely large value for electrons with mean energies near 1 eV. The pressure dependence indicated a linear increase in ν_{ca} with changes in n as predicted by our model. We conclude that collisions with

ground state molecules are responsible for the excitation transfer between the a and c states.

When we perturb the a state we see depletion signals in the c-state absorption signal of the same temporal form and of similar magnitude as for the reverse process shown in Figure 7. The similar time dependence is expected from the fact that in the case of $C_0 = 0$, Equation (6) for C(t) has the same form as Equation (9) but with a different yet similar magnitude factor, i.e., $A_0\nu_{ac}/(\alpha - \beta)$. The similar magnitudes for the depletion signals are due to the small energy difference between the two states, e.g., the energy difference between the v = 0, N = 1 levels is only 201 cm^{-1} and is approximately equal to kT of 208 cm^{-1}.

The measured fractional absorption changes in these collisional coupling experiments can be used to evaluate the rate coefficient for the energy transfer process. We begin by noting that for the small absorption values found in this experiment, the observed fractional changes in absorption $S_a(t)$ and $S_c(t)$ are related to the changes in excited state densities in our model by $S_c(t) = \sigma_c LC(t)$ and $S_a(t) = \sigma_a LA(t)$, where σ_c and σ_a are the absorption coefficients at line center for the transitions listed in Table 3 and L is the absorption path length. If $A_0 = 0$ and $C_0 \neq 0$ at t = 0, then $S_c^c = \sigma_c LC_0$, where the subscript indicates the state producing the absorption and the superscript indicates the state being perturbed by the pulsed laser. From fitting data such as that in Figure 7 to Equation (9), we obtain a value for S_a^c which in our model is given by $S_a^c = \sigma_a L\nu_{ca}C_0/(\alpha - \beta)$. The ratio of these two absorption values yields

$$\frac{S_a^c}{S_c^c} = \frac{\sigma_a \nu_{ca}}{\sigma_c(\alpha - \beta)} \qquad (10)$$

Table 3. Data used for analysis of collisional excitation transfer between v = 1, N = 1 levels of the $c^3\Pi_u^-$ and $a^3\Sigma_g^+$ states of H_2. The H_2 density was 2.1×10^{22} m^{-3} and the current was 1.5 A. The wavelengths are vacuum values.

Perturbed level			Observed level			Depletion ratios
state	λ(nm)	%dep.	state	λ(nm)	%dep.	from fitting
a	608.246	1.9	c	602.291	.056[a]	$S_c^a/S_a^a = 0.08$
c	602.291	1.6	a	608.246	.038[a]	$S_a^c/S_c^c = 0.067$

[a] These maximum values of the depletion waveforms are about one third of the amplitude factors obtained by fitting equations such as Equation (9) to waveforms such as in Figure 7 and used to calculate the ratios in the last column of this table.

Similarly, for $C_0 = 0$ and $A_0 \neq 0$ the ratio of the fitting constants obtained from the absorption data is

$$\frac{S_c^a}{S_a^a} = \frac{\sigma_c \nu_{ac}}{\sigma_a(\alpha - \beta)} \quad . \tag{11}$$

We now make use of detailed balancing[33] to obtain

$$\frac{\nu_{ca}}{\nu_{ac}} = K = \exp[-(\epsilon_a - \epsilon_c)/kT] \quad , \tag{12}$$

where ϵ_a and ϵ_c are the energies of the a and c states, k is Boltzmann's constant, and T is the gas temperature. In the present experiments K = 0.38.

Equations (10), (11), and (12) are next combined to yield

$$\nu_{ac} = k_{ac} n = |\alpha - \beta| \left[\frac{S_a^c}{S_c^c} \times \frac{S_c^a}{S_a^a} \times \frac{1}{K}\right]^{1/2} \quad . \tag{13}$$

Using the data of Table 3 and the measured α and β values in Equation (13), we calculate the excitation transfer rate coefficients to be $k_{ac} = (4 \pm 1) \times 10^{-16}$ m^3 s^{-1} and $k_{ca} = (1.5 \pm 0.3) \times 10^{-16}$ m^3 s^{-1}. The uncertainties assigned to these rate coefficients are estimates based on the statistical analysis of other data in this experiment, since only the one complete set of data shown in Table 3 was obtained with sufficient signal-to-noise ratio for the analysis. Although not small compared to usual values, these excitation transfer rate coefficients are small enough so that their contributions to Equations (4) and (5) can be neglected in experiments designed to measure the dominant loss process for the a state. Because of the limited amount of data, it is not possible to say whether the uncertainties in the excitation transfer coefficients allow transfer to account for all of the a-state collisional

destruction. In spite of this, we propose that excitation transfer is responsible for a state destruction via the c state.

Equations (10) to (13) and the data of Table 3 can also be used to obtain the ratio of the absorption coefficients at line center for the two lines used, i.e., $\sigma_c/\sigma_a = 0.7 \pm 0.2$. Time did not permit measurements of the type shown in Table 3 for the v = 0, N = 1 levels of the a and c states.

SECTION IV

N_2 a" $^1\Sigma_g^+$ METASTABLE DESTRUCTION AND COLLISIONAL COUPLING

The a" $^1\Sigma_g^+$ state of molecular nitrogen was first identified in the far ultra-violet absorption spectrum by Dressler and Lutz.[34] A Rydberg series of bands in the visible absorption spectrum was later identified by Ledbetter[35] as $c_4\ ^1\Pi_u \leftarrow$ a" $^1\Sigma_g^+$ transitions. This transition is shown in the term level diagram of Figure 8 and is the one used in our experiments. The Ledbetter band was first seen using optogalvanic techniques by Feldmann.[36] Later this technique was used for high resolution studies.[37] More recently high resolution VUV absorption spectroscopy has been used to obtain improved term values for the a" level.[38] Estimates of the radiative lifetime of the a"-state have been questioned.[39] The collisional destruction has as yet not been reported. Recently, various Russian authors[40] have proposed that the a"-state is responsible for multistep ionization and the growth of instabilities in high energy density N_2-CO_2 laser discharges.

The present work represents a study of the collisional quenching of the a"-state in a N_2 discharge by ground state molecular nitrogen. Also presented is a very brief study of the metastable $A^3\Sigma_g^+$ state (to be referred to as the A state) in the afterglow of the excitation pulse. Finally, we summarize attempts to measure the electric field strengths necessary to maintain the discharge and attempts to obtain consistency with discharge models.

A. Technique

Metastables in the a"-state were generated in a pulsed discharge and probed using the laser absorption technique described in Section II. This

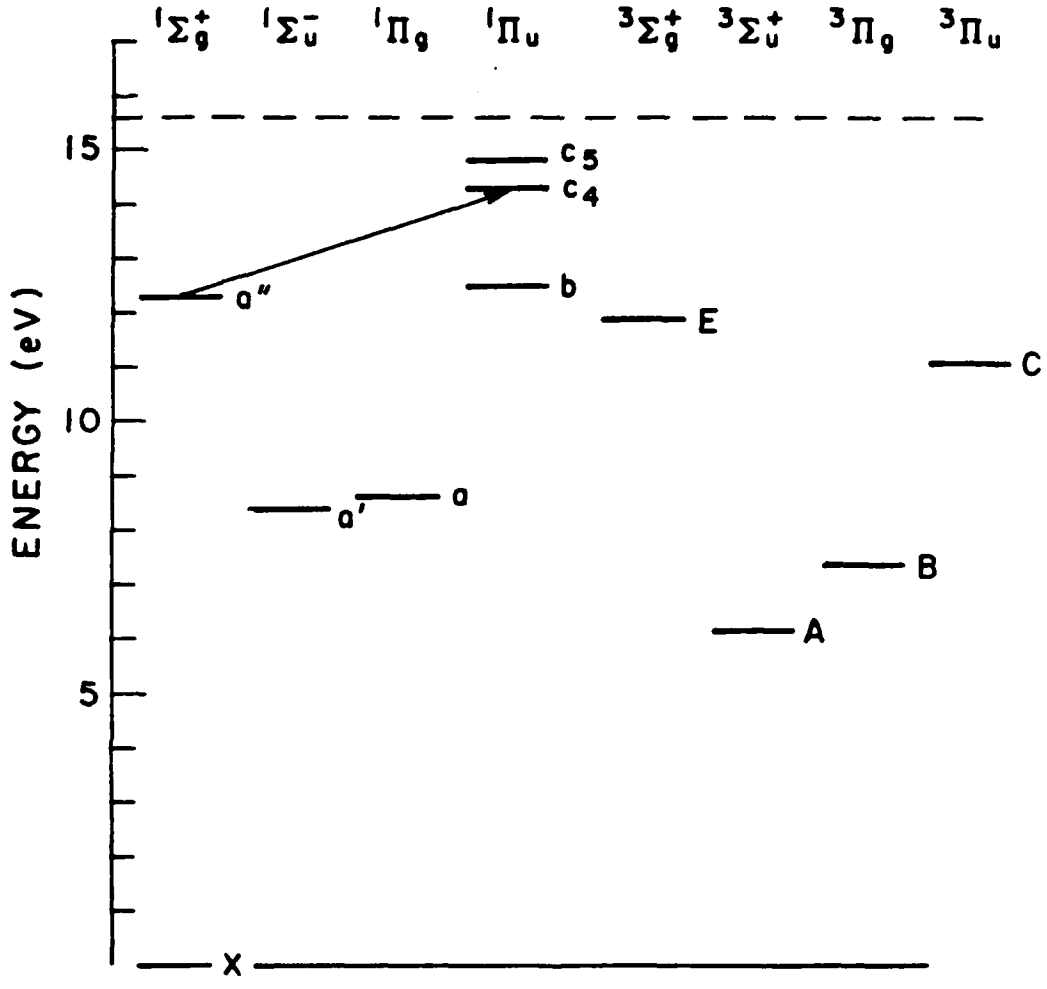

Figure 8. Energies of metastable and other levels of the N_2 molecule of interest in the present experiments. The arrow indicates the Ledbetter transition used to detect the a" $^1\Sigma_g^+$ metastables.

population was then perturbed by pulsed laser excitation and the collisional quenching rate determined from the recovery of population after the depletion. The discharge tube and optical system are the same as that shown schematically in Figure 1 and described in Section II.

Representative absorption and depletion waveforms are shown in Figure 9. These waveforms differ from those of Figure 4 for the $H_2(c^3\Pi_u^-)$ metastable in that for the N_2 a" metastable the absorption continues to decrease throughout the pulsed discharge and the time constant for the recovery of the a" population following laser-induced depletion is considerably longer than for the c state of H_2. For a typical discharge pulse the current increases to a nearly constant level in the first few μs. At the larger discharge currents the a"-state density, as shown by the absorption in the upper part of Figure 9, decays by over an order of magnitude. For lower currents (< 1 Amp) the a"-state density decreases more slowly than shown in Figure 9. For the collisional quenching experiments, low currents were used when possible in order to obtain minimize the change in a"-state density over the time of the measurement. To do this the a"-state density was perturbed by pulsed laser excitation in the last 2 μs of the discharge pulse. Typical discharge currents ranged from 0.6 to 1.5 A and gas densities from 6.5×10^{21} to 2.25×10^{22} m^{-3} (27 to 93 Pa).

Both the 2nd positive $C^3\Pi_u \rightarrow B^3\Pi_g$ emission at 337 nm and the 1st negative $B^2\Sigma_u^+ \rightarrow X^2\Sigma_g^+$ emission at 391 nm mimic the time dependence of the a"-density. We interpret this agreement as evidence that the time dependence of the production of the a", $C^3\Pi_u$, and $B^2\Sigma_u^+$ states follows the time dependence shown by the a"-state waveform. While the 1st positive $B^3\Pi_g(v=5) \rightarrow A^3\Sigma_u^+(v=2)$ emission waveform at 671 nm is lengthened significantly by the 6 μs lifetime

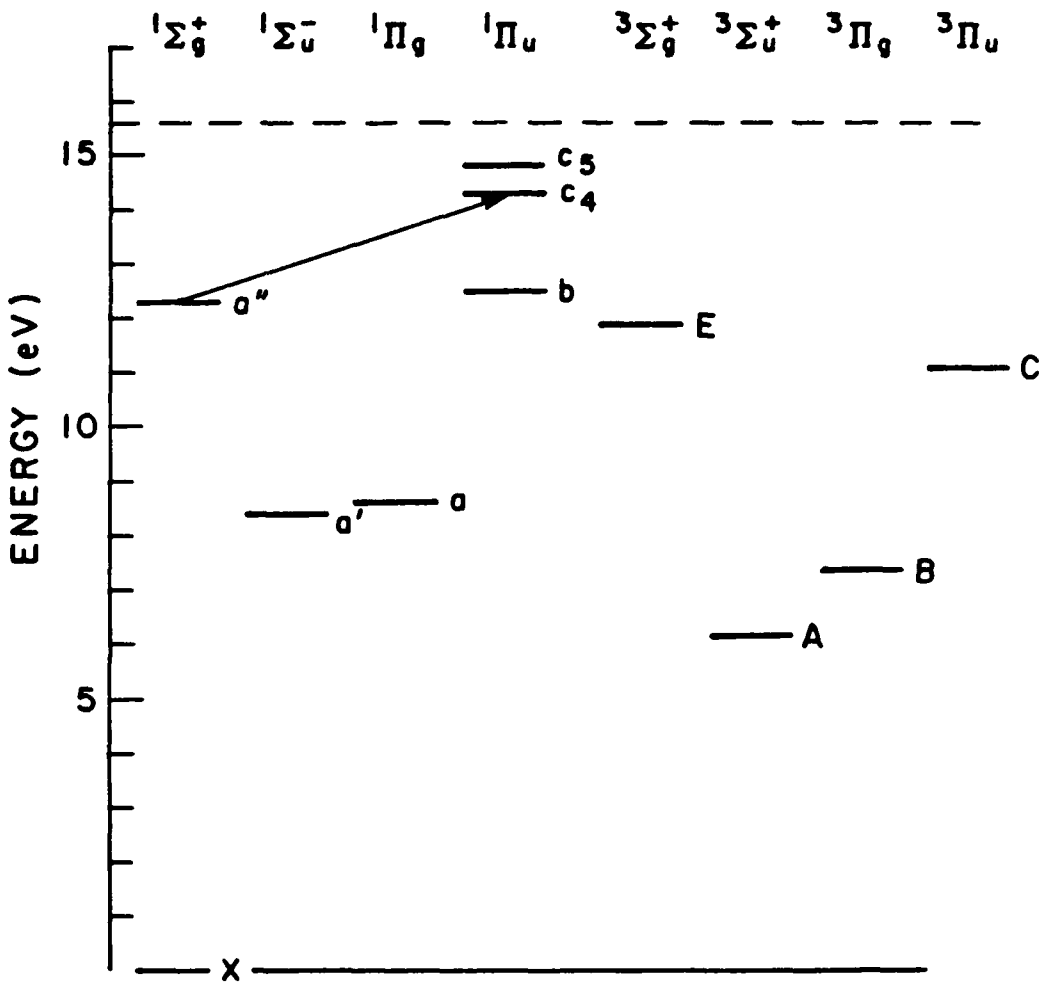

Figure 8. Energies of metastable and other levels of the N_2 molecule of interest in the present experiments. The arrow indicates the Ledbetter transition used to detect the a" $^1\Sigma_g^+$ metastables.

population was then perturbed by pulsed laser excitation and the collisional quenching rate determined from the recovery of population after the depletion. The discharge tube and optical system are the same as that shown schematically in Figure 1 and described in Section II.

Representative absorption and depletion waveforms are shown in Figure 9. These waveforms differ from those of Figure 4 for the $H_2(c^3\Pi_u^-)$ metastable in that for the N_2 a" metastable the absorption continues to decrease throughout the pulsed discharge and the time constant for the recovery of the a" population following laser-induced depletion is considerably longer than for the c state of H_2. For a typical discharge pulse the current increases to a nearly constant level in the first few μs. At the larger discharge currents the a"-state density, as shown by the absorption in the upper part of Figure 9, decays by over an order of magnitude. For lower currents (< 1 Amp) the a"-state density decreases more slowly than shown in Figure 9. For the collisional quenching experiments, low currents were used when possible in order to obtain minimize the change in a"-state density over the time of the measurement. To do this the a"-state density was perturbed by pulsed laser excitation in the last 2 μs of the discharge pulse. Typical discharge currents ranged from 0.6 to 1.5 A and gas densities from 6.5×10^{21} to 2.25×10^{22} m^{-3} (27 to 93 Pa).

Both the 2nd positive $C^3\Pi_u \rightarrow B^3\Pi_g$ emission at 337 nm and the 1st negative $B^2\Sigma_u^+ \rightarrow X^2\Sigma_g^+$ emission at 391 nm mimic the time dependence of the a"-density. We interpret this agreement as evidence that the time dependence of the production of the a", $C^3\Pi_u$, and $B^2\Sigma_u^+$ states follows the time dependence shown by the a"-state waveform. While the 1st positive $B^3\Pi_g(v=5) \rightarrow A^3\Sigma_u^+(v=2)$ emission waveform at 671 nm is lengthened significantly by the 6 μs lifetime

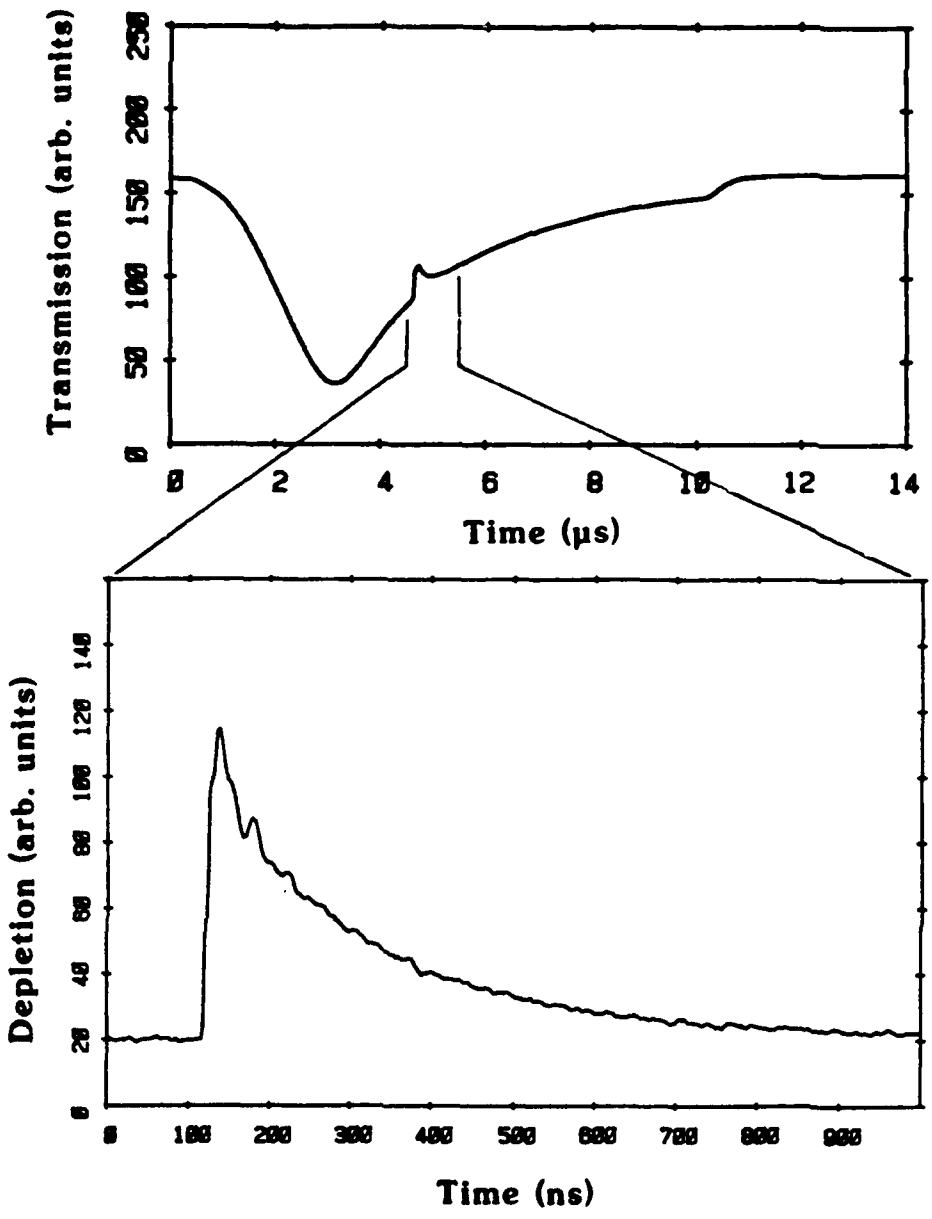

Figure 9. Upper trace: Absorption signal for the a" $^1\Sigma_g^+$(v = 0, J = 6) state resulting from the pulsed discharge in N_2. Lower trace: Magnified trace showing the depletion signal for the a" $^1\Sigma_g^+$(v = 0, J = 6) state resulting from excitation to the c_4 $^1\Pi_u$ state by the pulsed laser. This transient was taken using the multi-pass system and single mode operation of the cw laser.

of the upper state,[41] it also is consistent a production of the $B^3\Pi_g$ state which follows that of the a" state.

B. Absorption spectrum

A single-mode-laser absorption scan of the Q-branch bandhead of the Ledbetter $c_4\ ^1\Pi_u \leftarrow a"\ ^1\Sigma_g^+$ band is shown in Figure 10. The maximum absorption is about 2 percent. Allowing for the variation in incident intensity, the rotational distribution for the a" state peaks at J = 7 as does the ground state[42] at 300 K. The alternation in population for successive rotational levels[43] is also apparent, unlike the spectra obtained using optogalvanic techniques[37]. The Doppler broadened lines of the a"-state absorption spectra are clearly well separated from 1st positive transitions and individual rotational levels can be uniquely accessed. The Boltzmann population in v = 1 of the ground state at 300 K is 1.4×10^{-5} that of the v = 0 level and hence $c_4\ ^1\Pi_u \leftarrow a"$-state transitions for vibrational levels with $v \geq 1$ are not expected to be detected. The barely discernable peaks in this absorption spectrum are from the $\Delta v = 4$ transitions of the 1st positive $B^3\Pi_g \leftarrow A^3\Sigma_u^+$ system. The characteristics of the $A^3\Sigma_u^+$ signal will be discussed in Section IV E. Absorption by other systems such as the $\Delta v = 7$ "Y" bands and the Gaydon Green System[45] was not apparent in a multi-mode scan.

For the collisional quenching experiments discussed in this report, individual rotational lines in the Q-branch were probed using the cw laser while the same rotational level was perturbed on a Q, P, or R-branch transition. Because of their larger frequency spacing of use of the P and R branch transitions minimized the perturbation of neighboring rotational states due to the large linewidth of the pulsed laser. The linewidth of the single

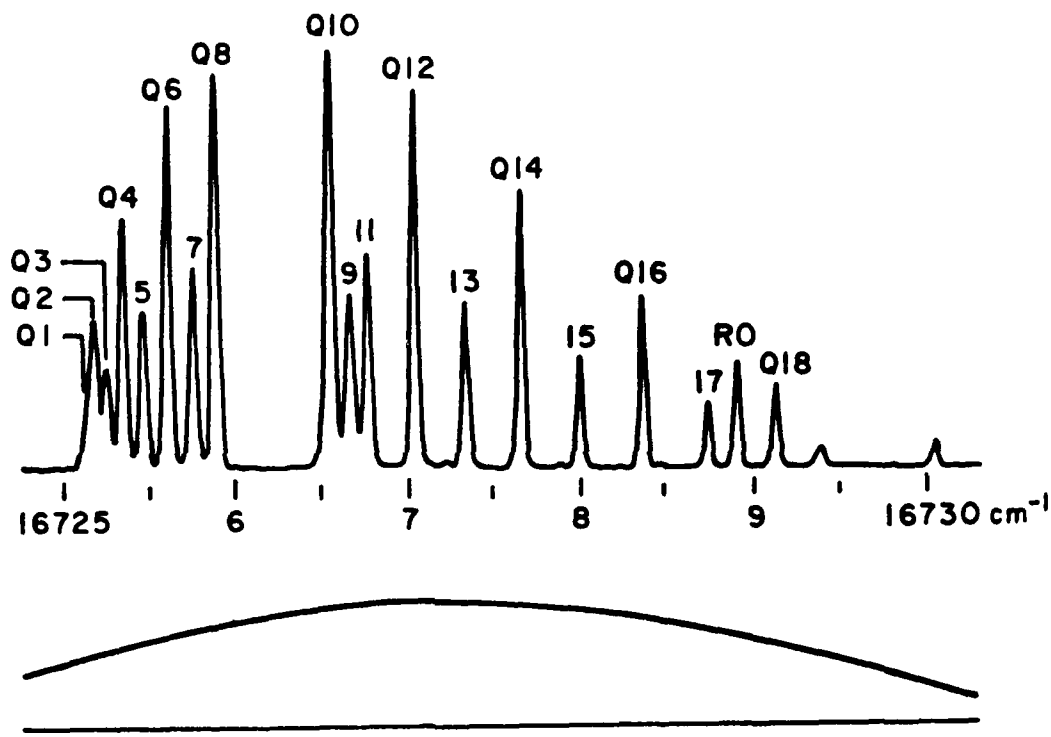

Figure 10. Absorption spectrum for the $c_4\ ^1\Pi_u \leftarrow a''\ ^1\Sigma_g^+$ transition (Ledbetter band) of N_2 (upper curve) and laser output versus wavelength (lower curve). The discharge current was 1 A and the N_2 density was $1.6 \times 10^{22}\ m^{-3}$.

mode cw laser was less than 50 MHz as measured by a 2 GHz free-spectral-range spectrum analyzer. The multimode pulsed laser linewidth as measured by scanning a Ne optogalvanic signal with a highly attenuated intensity was approximately 20 GHz.

C. $N_2(a'' \ ^1\Sigma_g^+)$ kinetics model

Pulsed laser depletion of the a"-state was timed to occur late in the discharge pulse in order to approach the quasi-equilibrium condition of constant electron excitation of the a" state. Under these conditions the time rate of change of the density of the J'th rotational level of the a" state n_J can be expressed by

$$dn_J(t)/dt = k_{eJ}n_e(T)n - \nu_a n_J(t) - A_J n_J(t) - \sigma F_J(t)[n_J(t) - rn_c(t)] - n_J \sum_{J'} \nu_{J,J'} + \sum_{J'} n_{J'} \nu_{J',J} \quad , \tag{15}$$

where k_{eJ} is the rate coefficient for electron excitation of N_2 to the J'th rotational level of the a" state, ν_a is the collisional destruction frequency to unspecified lower electronic states, A_J is the Einstein coefficient for spontaneous emission from the J'th level of the a"-state, $\nu_{J,J'}$ is the frequency of collisions which transfer excitation from the rotational level J to rotational level J', and σ is the effective cross section for the absorption of the pulsed laser flux $F_J(t)$ when tuned to the J'th level. The a"-state density is excited to the $c_4\Pi$ state of density n_c, and r is the statistical weight ratio for the levels. For the present discussion we will assume that ν_a and $A_J \equiv A_a$ are independent of J.

The set of equations represented by Equations (15) has been truncated at J = 16 and solved for J = 0 through 16 using a minicomputer program developed at NBS/Gaithersburg.[45] Examples of the solutions to Equations (15) in which the J = 6 level is perturbed and which give a qualitative fit to the experimental data presented in Section IV D are shown in Figure 11. In this particular case, the solution for the rotational level perturbed by the laser consists of a rapid decay of the perturbed level density caused by excitation transfer to adjacent rotational levels and a slower decay dominated by quenching to lower electronic states. The initially unperturbed levels show a relatively rapid increase in population cause by excitation transfer followed by the common slower decay by electronic-state quenching.

A special case of interest is that in which the variation of the pulsed laser flux $F(t)_J$ with wavelength and J is such that the distribution of perturbed rotational level densities is approximately the same as the steady state density distribution given by Equations (15). This situation is roughly that which occurs when the pulsed laser is adjusted for a wide spectral output and is tuned to the Q-branch transitions. In this case collisional mixing of the levels will not be observed and each of the levels will decay with the electronic quenching decay frequency, ν_a. The solution after the flux F(t) has decreased to zero is

$$n_J(t) = k_{eJ} n_e n/\nu_a' - \Delta A_J \exp(-\nu_a' t), \qquad (16)$$

where ν_a' is the total destruction frequency. Here ΔA_J is the change in density of J'th level of the a"-state as a result of pulsed laser excitation. The time constant for recovery of a"-state density is given by the reciprocal

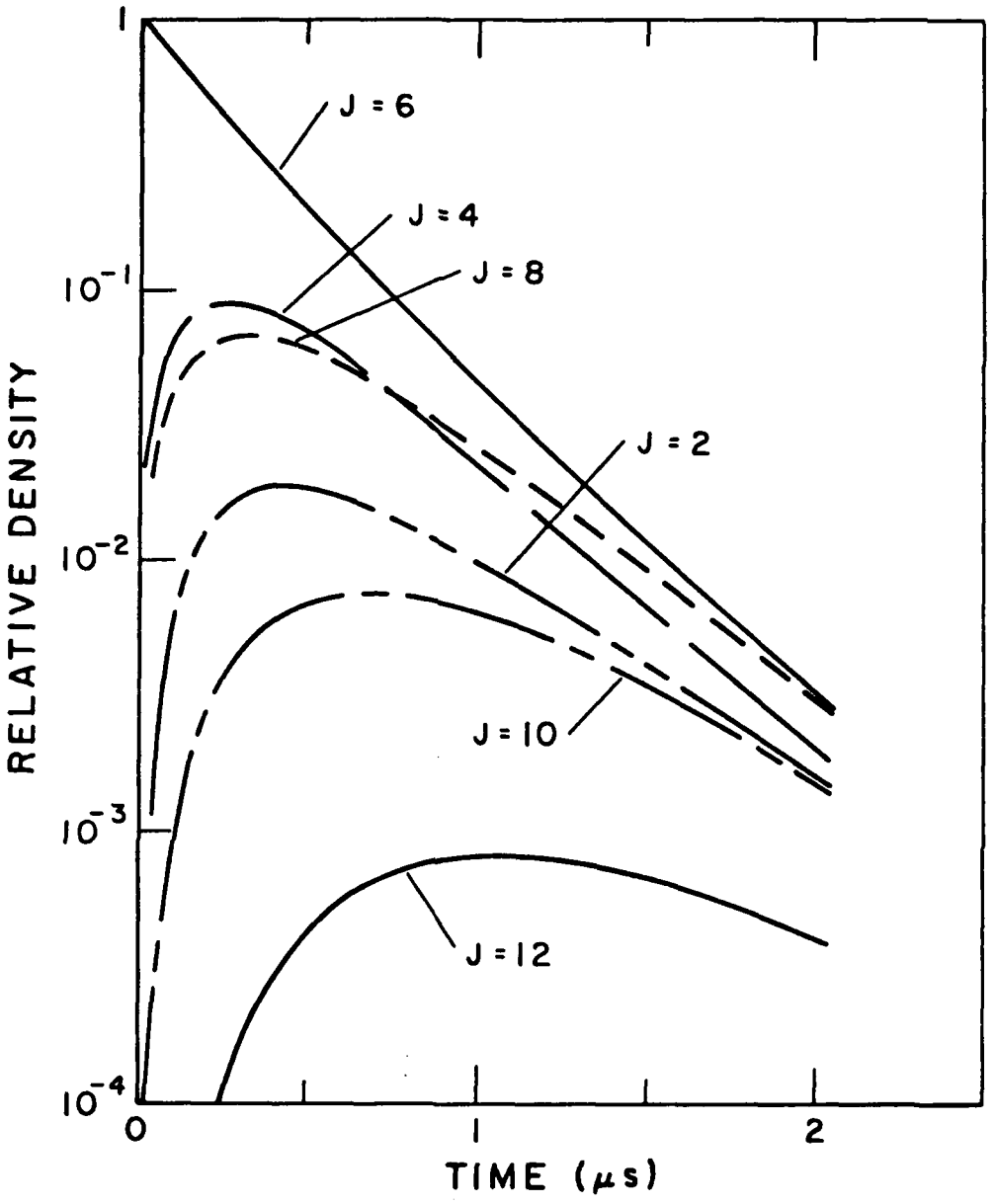

Figure 11. Calculated changes in relative density of various rotational levels of the a" $^1\Sigma_g^+$ state following laser perturbation of the J = 6 level population. The calculations used the set of equations represented by Equations (15) and rate coefficients chosen to approximate the data of Figure 14.

of the total destruction frequency ν_a', and can be obtained by a fit of a single exponential to the depletion transient. A typical depletion signal is shown in the lower part of Figure 9.

In order to obtain the collisional quenching rate coefficient k_{qa} depletion signals were obtained for a range of gas densities. The influence of gas heating and the effects of quenching by electrons, excited N_2 molecules, atomic nitrogen, and other products of the discharge was determined by measuring the total destruction frequency for a range of discharge currents. In order to carry out the separation of these effects, we express the total destruction frequency as

$$\nu_a' = bI + k_{qa}N + A_a. \qquad (17)$$

Here k_{qa} is the rate coefficient for collisional quenching of the various rotational levels of the a" state and by hypothesis is independent of J. We have assumed that the change in the destruction frequency caused by current dependent phenomena can be represented by a linear dependence on current. Equation (17) will be applied to the data of Section IV D.

D. $N_2(a'' \ ^1\Sigma_g^+)$ data

The depletion waveform shown in the lower portion of Figure 9 is representative the better data obtained in the early phases of these experiments. Although not shown, these waveforms yield a good fit to the single exponential predicted by Equation (16) for the case of pulsed laser perturbation of several nearby rotational levels. Although the details of the pulsed laser adjustment which produced these simple depletion waveforms were

not recorded, we will assume that the measured decay frequencies ν_a' are characteristic of the common decay of the collisionally coupled rotational levels of the a" state. This assumption has been shown to be consistent with the data obtained in which it was demonstrated that only one rotational level was depleted. See the discussion at the end of this section.

A small current dependence in the destruction of the a" state was observed and the results for the J = 6 level are shown in Figure 12. Here we have plotted ν_a' versus the discharge current I. The points shown are averages of approximately 5 to 8 measurements for each current.

The dependence of the J = 6 a"-state destruction frequency on N_2 density is shown in Figure 13. According to Equation (17), the slope of the destruction frequencies versus the N_2 density determines the collisional quenching coefficient k_{qa} to be 2×10^{-16} m^3/s. The intercept at zero gas density gives the sum of the current dependent term and the radiative decay constant, i.e., $bI + A_a$. Since the current dependence of Figure 12 yields a correction at 0.6 A of $(0.6 \pm 0.1) \times 10^6$ s^{-1} and the zero density intercept is $(0.8 \pm 0.2) \times 10^6$ s^{-1}, the apparent radiative lifetime of the a"(v=0, J=6) level is $5 \pm 5\mu s$. In view of the present uncertainties in the experiment, we make no claims to have measured A_a.

Time constants for recovery of the a"-state density were taken at times ranging from the peak in absorption shown in Figure 9 to within 1 μs of the end of the pulse. No change in ν_a' was observed within the uncertainty of the measurements, which means that k_{qa} is constant. During this period the a"-state absorption and density is decreasing by as much as an order of magnitude, while the discharge current is nearly constant. Since the a"-state

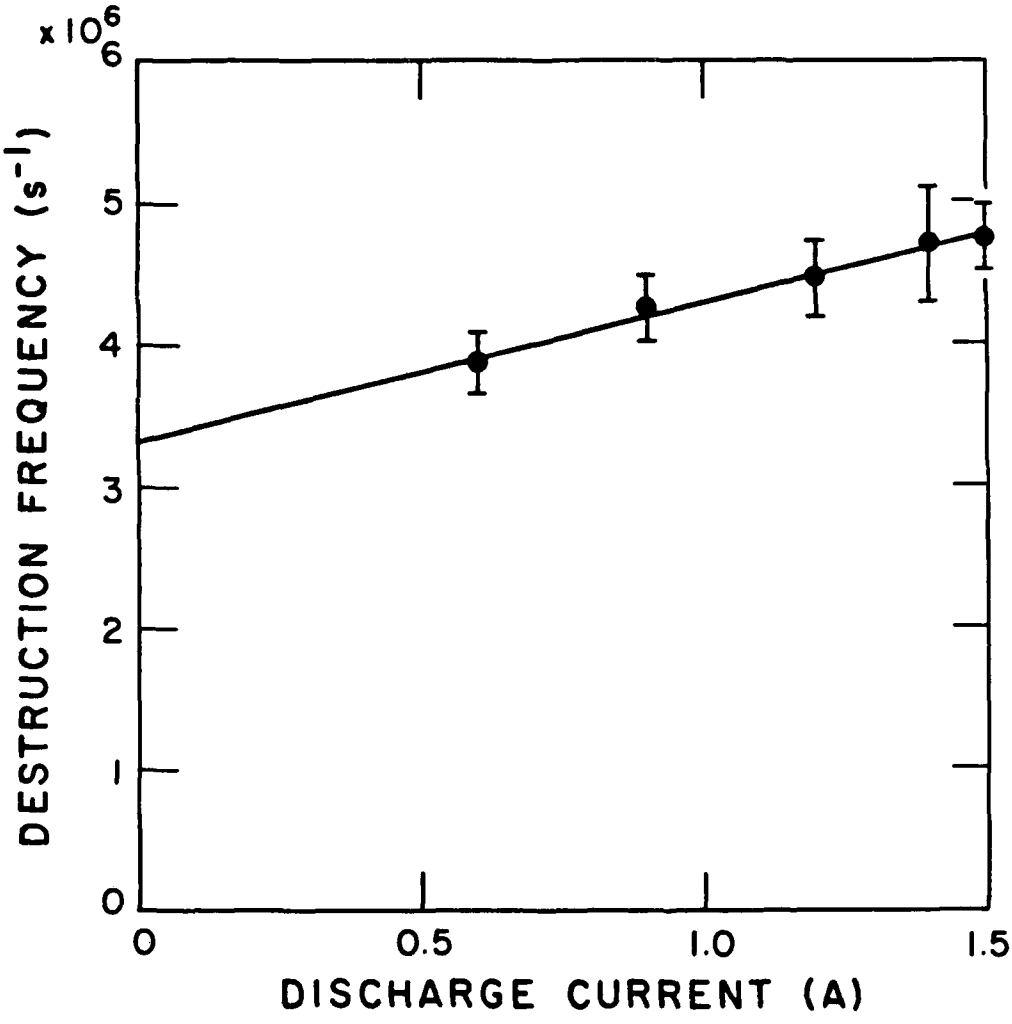

Figure 12. Destruction frequencies for the J = 6 level of the a" $^1\Sigma_g^+$ state versus discharge current for an N_2 density of 1.6×10^{22} m^{-3}.

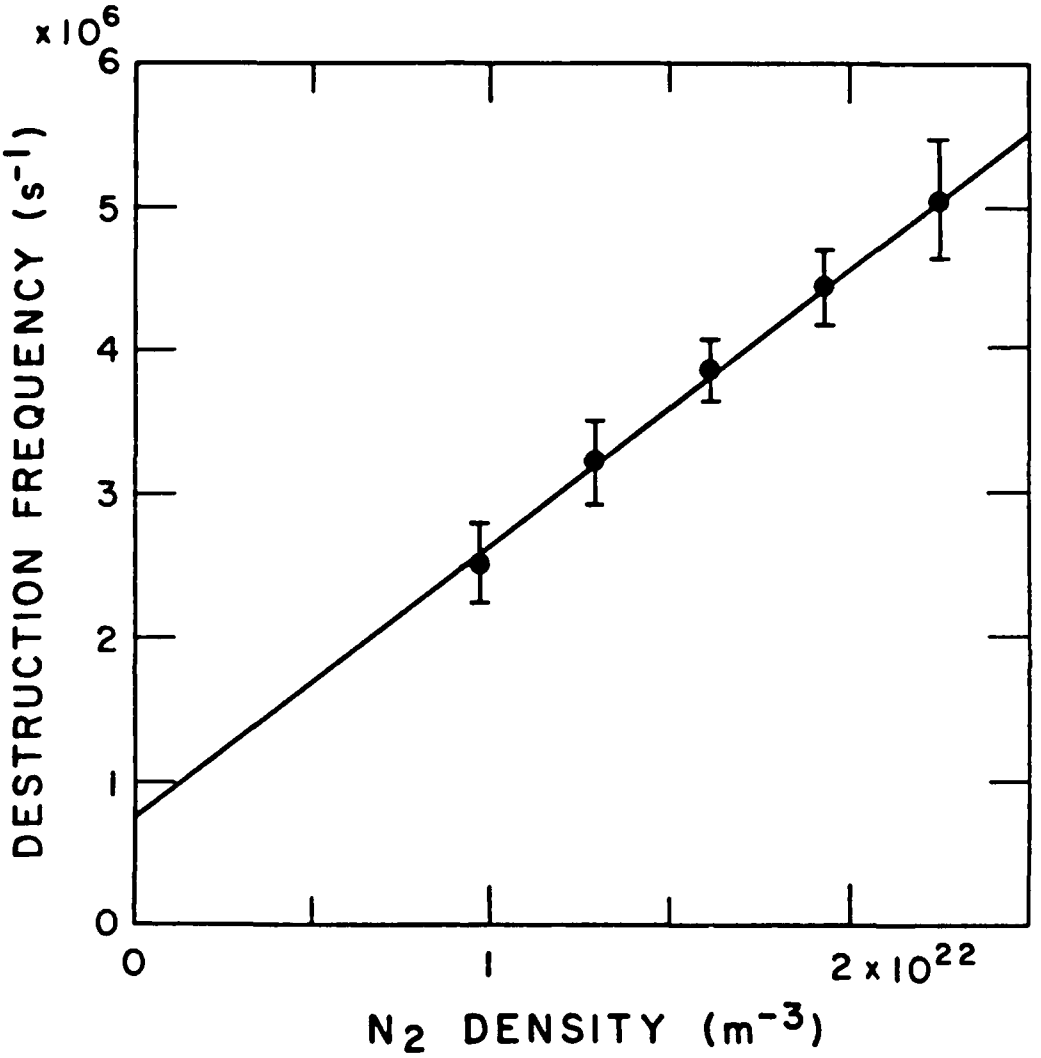

Figure 13. Destruction frequencies for the J = 6 level of the a" $^1\Sigma_g^+$ state versus N_2 density for a discharge curent of 0.6 A.

lifetime is short compared to the time scale of these changes, the appropriate quasi-steady-state balance is

$$k_{eq} n_e N = k_{qa} n_a N, \tag{18}$$

where n_e is the electron density and n_a is the a"-state density. It therefore appears that the electron excitation rate coefficient for the a" state k_{ea} is a rapidly decreasing function of time.

Figure 14 shows an example of data in which the pulsed laser was tuned to the J = 6 level of the R branch so as to insure that only one rotational level was perturbed. This data appears to confirm the model in which the collsional coupling between rotational levels is primarily by $\Delta J = 2$ transitions and the final destruction rate coefficient is somewhat smaller than the coupling rate coefficients. Although no quantitative fitting of the model this data had been attempted at the end of this report period, the constants used in the model calculations of Figure 11 were chosen to give rough agreement with this experimental data. Obviously, further work is necessary to obtain rate coefficients characteristic of the collisional coupling and electronic destruction.

E. $A^3\Sigma_g^+$ destruction

It is generally agreed[46] that the radiative lifetime of the metastable $A^3\Sigma_g^+(v = 0)$ level is a approximately 2 s. Significant absorption was seen for the $\Delta v=4$ transitions of the 1st positive system, indicating significant populations of the higher lying vibrational levels of the A-state late in the discharge pulse. In fact, the density peaks approximately 30 μs after the

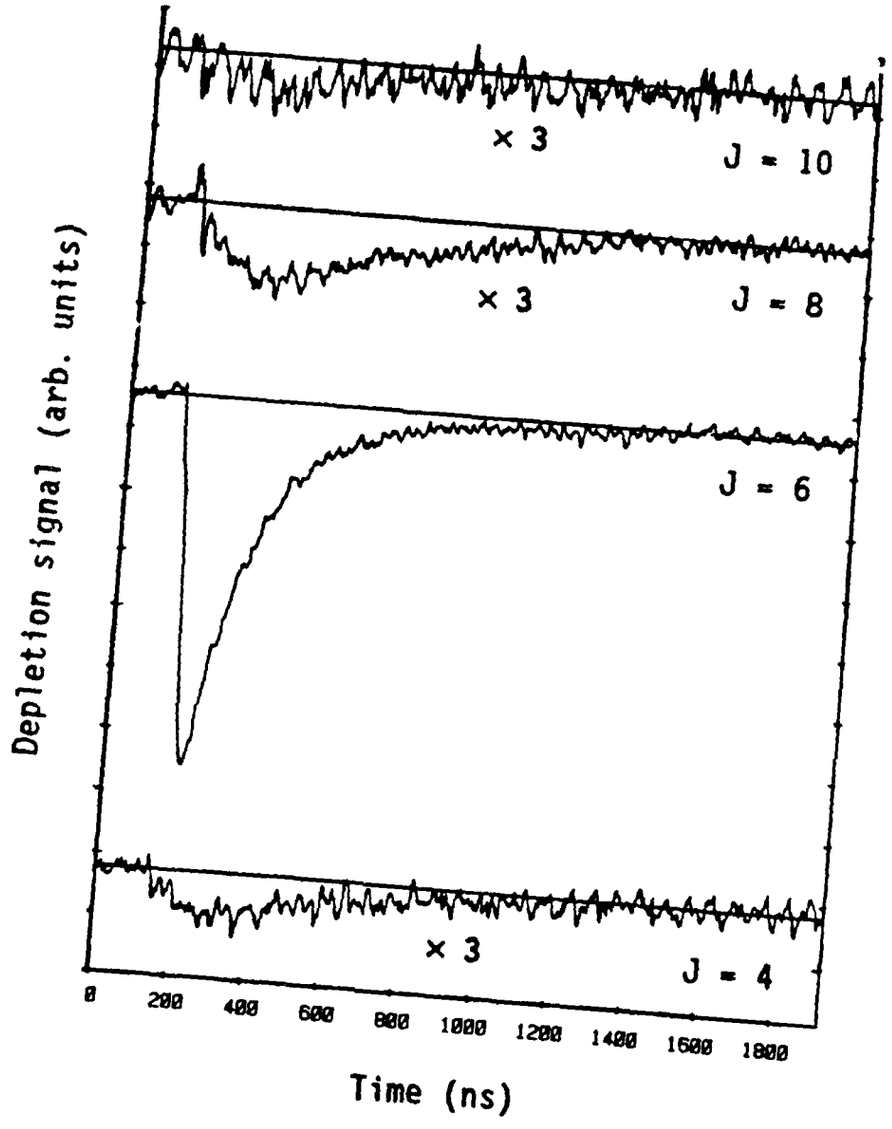

Figure 14. Experimental changes in relative density of various rotational levels of the a" $^1\Sigma_g^+$ state following laser perturbation of the J = 6 level population. The measurements were made for a N_2 density of 1.5×10^{22} m^{-3} and a discharge current of 1 A.

discharge pulse is initiated for the experimental conditions discussed in Figure 9. The population then decreases exponentially with time. We have looked at the variation in A-state decay with vibrational level for lines near the band head of each $\Delta v = 4$ transition.[44] The decay rate of these higher lying vibrational levels is extremely rapid compared to the radiative decay rate of the v=0 level. Insufficient decay constant data was obtained to be discussed further.

F. Electric field determinations

Voltage waveforms measured using high impedance probes at two positions in the positive column of the discharge are shown in Figure 15. Also shown are absorption and current waveforms. The voltage difference waveform shows that for the conditions of Figure 15, E/n decreases about 10 percent during the period from 12 to 16 μs, while the current increases about 10 percent. The absorption waveform shows a factor of 2.7 decrease during this time. We find (Section IV A) that the destruction of the a"-state is independent of time during the discharge pulse. These observations and the application of Equation (18) implies that the rate coefficient for electron excitation of the a" state is decreasing by about a factor of three during the 12 to 16 μs period. This result is inconsistent with the small change in E/n, since the calculated chenge in the electron excitation rate coefficient is only about a factor of 1.5. The hypothesis of a changing excitation coefficient with time is supported by the observation that the emission of radiation by short lived excited states of N_2 have a similar time dependence to the a" state absorption. The voltage probe results were checked by measuring the cathode voltage waveform for two lengths of the discharge tube using the two anodes

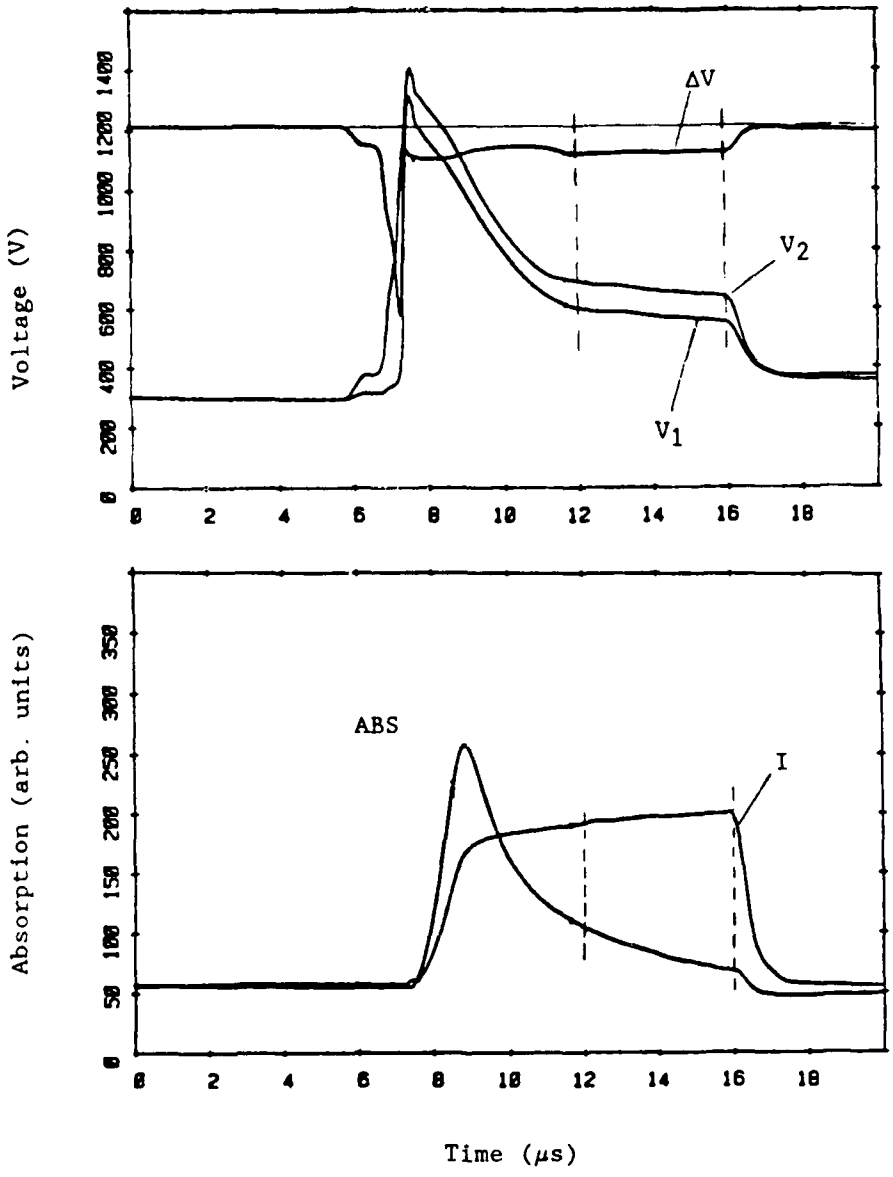

Figure 15. (a). Voltage waveforms obtained using fine-wire Langmuir probes near the discharge tube wall were separated by 50 mm. V_1 and V_2 are from probes 1 and 2. ΔV is their difference. (b). Absorption and current waveforms are marked ABS and I, respectively. All are for a pressure of 0.5 Torr and a peak current was 1.5 A.

shown in Figure 1. Although there was a significant discrepancy between magnitudes of the electric fields derived from the two techniques, the difference voltages show comparable decreases in E/n during the later stage of the discharge. Obviously these experiments need to be repeated and extended to other pressures, etc.

Representative electric field determinations using the double-anode techniques yield the E/n versus nR data shown by the points in Figure 16. The points were obtained using the change in discharge voltage with length. The smooth curve shows E/n values calculated by balancing the production of electrons and ions by electron impact ionization of N_2 against the loss by ambipolar diffusion.[47] In this calculation we used the ionization, diffusion, and drift velocity data for electrons of Wedding, Blevin, and Fletcher.[48] We assumed the ions to be N_2^+ and used the thermal mobility data of Ellis et al.[49] The discrepancy is significantly larger than that we found[3] previously for similar pulsed discharges in H_2. The reason for the discrepancy in N_2 discharges is unknown. One aspect of these discharges not yet investigated is the dependence of the E/n on the discharge current.

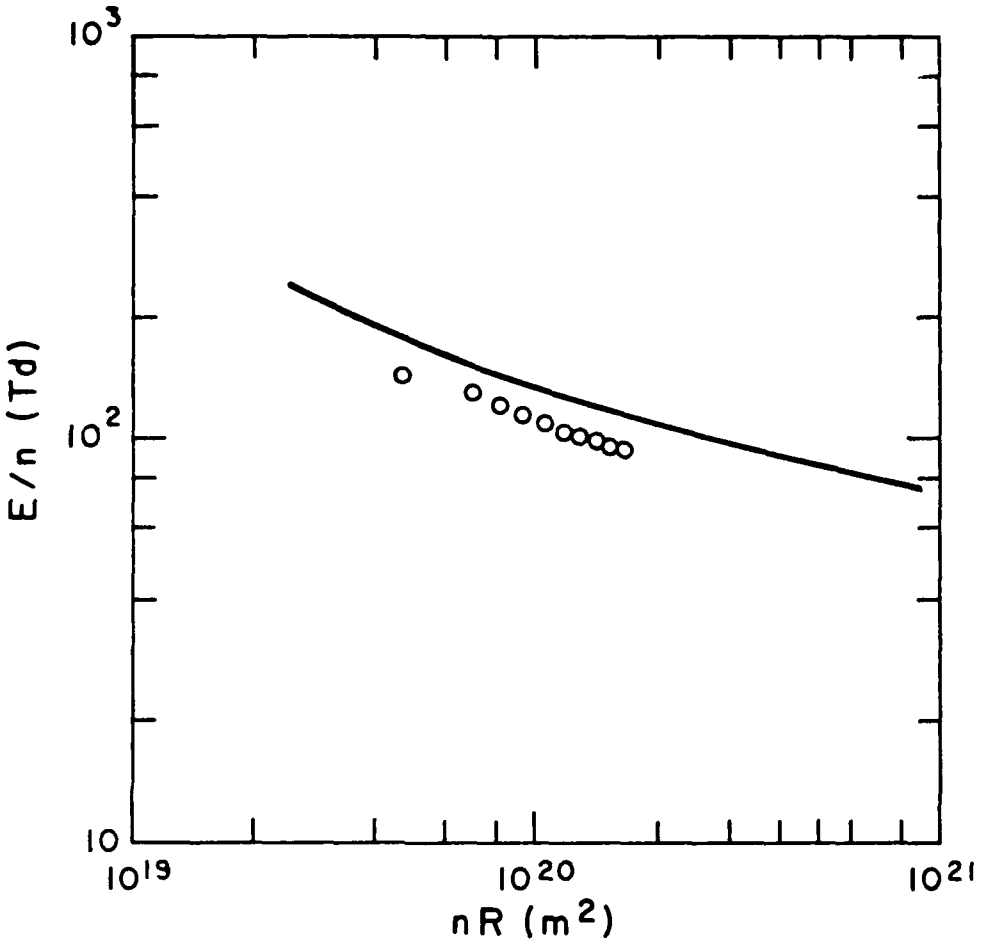

Figure 16. Experimental and calculated E/n values vs nR values for constant-current (1.5 A), pulsed discharges in N_2. The data shown by the open circles were obtained at about 5 μs after the beginning of the discharge from the change in cathode voltage when the length of the discharge was varied 50 mm. The curve was calculated as discussed in the text.

SECTION V

CONCLUSIONS

The laser absorption technique used in this work has been shown to be a useful and versatile tool for the study of the collisional and radiative properties of excited molecular hydrogen and nitrogen in metastable and radiating states. The technique has been found valuable both in the variety of parameters that can be investigated and in its ability to uniquely select vibrational and rotational levels for study.

The interaction of the $H_2(a^3\Sigma_g^+)$ molecules with ground state H_2, on the other hand, appears to result primarily in excitation transfer to the c state. The significantly lower rate coefficient suggests the possibility of a repulsive interaction between the a state and the $X^1\Sigma_g^+$ ground state and rather different temperature dependence of the destruction rate coefficients for the c and a states. On the other hand, the very large average cross section of 75 x 10^{-20} m^2 would seem to require that a long range (~ 0.5 nm) attractive potential surface(s) dominate the $H_2(c^3\Pi_u^-)$-$H_2(X^1\Sigma_g^+)$ interaction. Except for the correlation and energy level diagrams of Jungen and Staemmler,[16] the available calculations of potential surfaces are for singlet states. Similar large quenching cross sections have been reported for singlet states of hydrogen[32] and states with an ionic character are invoked.[33]

The large collisional quenching rate coefficient of 1.9 x 10^{-15} m^3 s^{-1} found for the $c^3\Pi_u^-$ states means that in electrical discharges at pressures above about 500 Pa (4 Torr) the $c^3\Pi_u^-$ levels will have a density comparable with or less than that of the $a^3\Sigma_g^+$ radiating state. The collisional coupling of the $c^3\Pi_u$ and $a^3\Sigma_g$ states is too slow to keep the populations of these

states in thermal equilibrium. The c state will therefore not be a particularly effective energy storage level in hydrogen discharges at high H_2 densities.[11] Similarly, the $c^3\Pi_u^-$ and $a^3\Sigma_g^+$ states may well make comparable contributions to multistep ionization and other electron-excited state collision processes in high current switches, negative ion sources, and infrared lasers.

Low intensity laser absorption has been successfully used to monitor selected rovibrational levels of the high lying metastable a"-state of molecular nitrogen. Pulse laser perturbation of this state yielded determinations of the rate coefficients for quenching by neutral ground state molecules. While the collisional quenching is not extremely rapid, it is however the dominant decay mechanism for the a" state in weakly ionized discharges, such as used for N_2-CO_2 lasers.

Measurements of E/n values for a range of N_2 densities gave results which were about 20 percent below theoretical predictions. However, since the two techniques used were in disagreement as to the time variation of the electric field, we must regard the results as preliminary. Furthermore, we are unable to satisfactorily explain the variation with time during the pulsed discharge of the density of metastables in the a" state of N_2.

REFERENCES

1. H. Tischer and A. V. Phelps, Chem. Phys. Lett. 117, 550 (1985).

2. A.B. Wedding and A.V. Phelps, J. Chem. Phys. (submitted) (1988).

3. A.B. Wedding and A.V. Phelps, Air Force Wright Aeronautical Laboratories Report AFWAL-TR-86-2113, April 1987.

4. D.S. Bethune, J.R. Lankard and, P.P. Sorokin, J. Chem. Phys. 69, 2076 (1973).

5. L.N. Breusova, Zh. Tekh. Fiz. 39, 1143 (1969)[Sov. Phys.-Tech. Phys. 14, 862 (1969)].

6. S.J. Buckman and A.V. Phelps, J. Chem. Phys. 82, 4999 (1985); S.J. Buckman and A.V. Phelps, JILA Information Center Report No. 27 (unpublished).

7. This estimate is based on 2.6 percent of the energy to elastic recoil heating and less than one-half of the 44 percent to electronic excitation to translational energy of dissociation. Rotational relaxation to translation can be neglected during our pulsed discharges. See R.J. Gallagher and J.B. Fenn, J. Chem. Phys. 60, 3492 (1974).

8. C.H. Muller, Jr., E.R. Mosburg, Jr., M.A. Islam, and A.V. Phelps (unpublished).

9. J.L. Hall and S.A. Lee, Appl. Phys. Lett. 29, 367 (1976); F. V. Kowalski, R.T. Hawkins, and A.L. Schawlow, J. Opt. Soc. Am. 66, 965 (1976).

10. A. Ernest, S.C. Haydon and M.T. Eld, Aust. J. Phys., 39,479 (1986).

11. W. Lichten, Phys. Rev. 120, 848 (1960); G. Herzberg, Science of Light, 16, 14 (1967).

12. C.E. Johnson, Phys. Rev. A 5, 1026 (1972); B. Meierjohann and M. Vogler, Phys. Rev. A 17, 47 (1978).

13. R.P. Freis and J.R. Hiskes, Phys. Rev. A 2, 573 (1970).

14. D.K. Bhattacharyya and L-Y. Chow Chiu, J. Chem. Phys. 67, 572/ (1977); L-Y. Chow Chiu and D.K. Bhattacharyya, J. Chem. Phys. 70, 4376 (1979).

15. R.T. Thompson and R.G. Fowler, J. Quant. Spectrosc. Radiat. Transfer 12, 117 (1972); J. Godart and V. Peuch, Chem. Phys. 46, 23 (1980).

16. K.A. Mohamed and G.C. King, J. Phys. B 12, 2809 (1979). See also G.C. King, F.H. Read, and R.E. Imhof, J. Phys. B. 8, 665 (1975)

17. H.M. James and A.S. Coolidge, Phys. Rev. 55, 184 (1939); T.L. Kwok, S. Guberman, A. Dalgarno, and A. Posen, Phys. Rev. A 34, 1962 (1987).

18. T.J. Morgan, K.H. Berkner, and R.V. Pyle, Phys. Rev. A 5, 1591 (1972).

19. J.M. Breare and A. VonEngel, Proc. Roy. Soc. A 282, 390 (1964); R.E. Center, J. Chem. Phys. 54, 3499 (1971).

20. W.B. McKnight and T.A. Barr, Appl. Optics, 41, 357 (1982); T.A. Barr and W.B. McKnight, Appl. Phys. Lett. 41, 114 (1982); I. Dabrowski and G. Herzberg, Acta Phys. Hung. 55, 219 (1984).

21. M.A. Gunderson and S. Guha, J. Appl. Phys. 53, 1190 (1982); S. Guha, J. A. Kunc, and M.A. Gundersen, IEEE J. Quantum Electron. QE-13, 504 (1984).

22. D.P. De Bruijn, J. Neuterboom, and J. Los, Chem. Phys. 85, 233, (1984).

23. H. Helm, D.P. De Bruijn, and J. Los, Phys. Rev. Lett. 53, 1642 (1984); H. Helm, in Electronic and Atomic Collisions, edited by D. C. Lorents, W. E. Meyerhof, and J.R. Peterson (Elsevier, B. V., 1986), p. 705. For an alternate notation see G. Herzberg, Spectra of Diatomic Molecules (Van Nostrand, New York, 1939), p. 239.

24. S. Chung and C.C. Lin, Phys. Rev. A 17, 1874 (1978); L. Mu-Tao, R.R. Lucchese, and V. McKoy, Phys. Rev. A 26, 3240 (1982); M.A. Khakoo and S. Trajmar, Phys. Rev. A 34, 146 (1986); N.J. Mason and W.R. Newell, J. Phys. B 19, L587 (1986).

25. M. Jungen and V. Staemmler, Chem. Phys. Lett. 103, 191 (1983).

26. C. Bottcher and B.D. Buckley, J. Phys. B, 12, L497 (1979). See also J. R. Hiskes, A.M. Karo, M. Bacal, A.M. Bruneteau and W.G. Graham, J. Appl. Phys. 53, 3469 (1982);

27. H.M. Crosswhite, The Hydrogen Molecule Wavelength Tables of Gerhard Heinrich Dieke (Wiley, New York, 1972) pp. T260-T319.

28. E.E. Eyler and F.M. Pipkin, Phys. Rev. Lett. 47, 1270 (1981).

29. B.P. Lavrov and D.K. Otorbaev, Opt. Spektrosk. 45, 1074 (1978) [Opt. Spectrosc. (USSR) 45, 859 (1978)]; T. Kiyoshima, Phys. Soc. Japan 56, 1989 (1987).

30. H. Tischer and A.V. Phelps (unpublished).

31. S.A. Lawton and A.V. Phelps, J. Chem. Phys. 69, 1055 (1978).

32. T.C. English and D.L. Albritton, J. Phys. B 8, 2123 (1975).

33. J.B. Tatum, Astrophys. J. Suppl. 16, 21 (1967).

34. K. Dressler and B.L. Lutz, Phys. Rev. Lett., 19, 1219 (1967).

35. J. W. Ledbetter, J. Mol. Spect., 42, 100 (1972).

36. D. Feldmann, Optics Comm., 29, 67 (1979).

37. T. Suzuki, Optics Comm., 38, 364 (1981); T. Suzuki and M. Kakimoto, J. Mol. Spect., 93, 423 (1982); M. Miyazaki, H. Scheingraber and C. R. Vidal, Phys. Rev. Lett., 50, 1046 (1983).

38. K. Yoshino and D. E. Freeman, Can. J. Phys., 62, 1478 (1984).

39. S. W. Sharpe and P. M. Johnson, J. Chem. Phys., 85, 4943 (1986).

40. L.S. Polak, I.A. Grishina, K.S. Kovalev, Teplofiz. Vys. Temp. 15, 13 (1977)[High Temperature 11, 13 (1977)]; Yu.B. Golubovskii and V.M. Telezhko, Teplofiz. Vys. Temp. 22, 428 (1983)[High Temperature 22, 340 (1983)];Yu.S. Akishev, K.V. Baiadze, V.M. Vetsko, A.P. Napartovich, S.V. Pashkin, V.V. Ponomarenko, A.N. Starostin, and N.I. Trushkin, Fiz. Plasmy 11, 999 (1985)[Sov. J. Plasma Phys. 11, 582 (1985)].

41. D. C. Cartwright, J. Geophys. Res., 83, 517 (1978).

42. K. Becker, J. L. Forand, P. W. Zetner and J. W. McConkey, J. Phys. B, 17, L915 (1984).

43. K. L. Carleton, K. H. Welge and S. R. Leone, Chem. Phys. Lett., 115, 492 (1985).

44. S. N. Suchard and J. E. Melzer, Spectroscopic Constants for Selected Homonuclear Diatomic Molecules, Report SAMSO-TR-76-31, Vol. II.

45. W. Braun, J.T. Heron, and D.K. Kahaner, Int. J. Chem. Kinetics (submitted) (1987).

46. N. P. Carleton and O. Oldenberg, J. Chem. Phys., 36, 3460 (1962); E. C. Zipf, J. Chem. Phys., 38, 2034 (1963); H. H. Brömer and F. Spieweck, Planet. Space Sci., 15, 689 (1967); D. E. Shemansky and N. P. Carleton, J. Chem. Phys., 51, 682 (1969); D. E. Shemansky, J. Chem. Phys., 51, 689 (1969).

47. M.J. Druyvestyen and F.M. Penning, Rev. Mod. Phys. 12, 87 (1940).

48. A.B. Wedding, H.A. Blevin, and J. Fletcher, J. Phys. D 18, 2361 (1985).

49. H.W. Ellis, R.Y. Pai, E.W. McDaniel, E.A. Mason, and L.A. Viehland, Atomic Data and Nuclear Data Tables 17, 177 (1976).

☆ U.S. GOVERNMENT PRINTING OFFICE: 1988 – 548-054-80956